Research on Chemical Intermediates
https://doi.org/10.1007/s11164-019-03765-9

Anti-cancer, anti-oxidant and molecular docking studies of thiosemicarbazone indole-based derivatives

Zohreh Bakherad[1] · Maliheh Safavi[2] · Afshin Fassihi[1] · Hojjat Sadeghi-Aliabadi[1] · Mohammad Bakherad[3] · Hossein Rastegar[4] · Jahan B. Ghasemi[5] · Saghi Sepehri[6] · Lotfollah Saghaie[1] · Mohammad Mahdavi[7]

Received: 13 December 2018 / Accepted: 30 January 2019

Abstract

Based on the structural elements of bioactive 3-substituted indoles, a new series of indole–thiosemicarbazone hybrid derivatives were designed, synthesized, and well-characterized using different spectral techniques. The intended scaffolds were screened for their in vitro anti-proliferative activities against breast cancer (*MCF-7*), lung cancer (*A-549*), and liver cancer (*Hep-G2*) cell lines, as well as their anti-oxidant properties. Cytotoxicity studies revealed that compound **6n** was the most potent, at least threefold more potent than the commercially available reference drug etoposide, against *A-549*. In addition, morphological analysis by the acridine orange/ethidium bromide double staining test and flow cytometry analysis confirmed induction of apoptosis in the *A-549* cells by compound **6n**. In order to validate the experimental results, molecular studies were performed to achieve the possible binding interactions of the most potent compound (**6n**) and colchicine with tubulin as well as ANP with ATPase domain of topoisomerase IIα active sites. Moreover, the radical scavenging potential of the final derivatives was found to be excellent with the range of 0.015–0.630 μM, comparable to the standard ascorbic acid (0.655 μM).

Keywords Indole · Thiosemicarbazone · Anti-oxidant · Anti-cancer · Apoptosis · Flow cytometry

This paper is dedicated to the memory of our wonderful teacher in Chemistry and Medicinal Chemistry, Professor Abbas Shafiee (1937–2016).

Electronic supplementary material The online version of this article (https://doi.org/10.1007/s11164-019-03765-9) contains supplementary material, which is available to authorized users.

✉ Lotfollah Saghaie
saghaie@pharm.mui.ac.ir

✉ Mohammad Mahdavi
momahdavi@tums.ac.ir

Extended author information available on the last page of the article

Published online: 27 February 2019

Introduction

Cancer is a class of diseases in which a group of cells demonstrate incontrollable growth, influx, and sometimes metastasis [1]. After cardiovascular disease, cancer is the second leading cause of mortality [2]. Although chemotherapy is among the main remedy options for cancer treatment, the use of available chemotherapeutics has limitations due to undesirable adverse effects and multi-drug resistance [3]. Therefore, the design and discovery of more effective and safer anti-cancer drug candidates have recently received great attention [4]. Molecular hybridization by a combination of different pharmacophores is a strategy for targeting two or more different receptors or enzymes to increase the efficacy [5]. Thus, a single molecule with more than one pharmacophore displaying diverse modes of action could be more useful in cancer treatment [6]. These drugs have the potential to overcome the fast progress of resistance, elevate patient admission, and reduce both the cost and risk of drug–drug interactions [7]. Heterocyclic compounds are an exceedingly important class of compounds, and they have attracted increasing attention for diverse biological studies [8–14].

Indole is a heterocyclic scaffold with various valuable biologic activities such as anti-inflammatory [15], anti-viral [16], anti-depressant, anti-hypertensive, anti-hypoglycemic [17], and notably anti-cancer properties [18–21]. The indole ring system is present in various marketed drugs [22]. Angerer's research group have designed and reported some analogs of 3-formyl-2-phenylindoles with the most potent one, **A**, which displayed IC_{50} values of 35 nM and 1.5 μM for cell growth and tubulin polymerization inhibition, respectively (Fig. 1) [23]. Prompted by these results, Kaufmann et al. synthesized a number of 2-phenyl indole-3-carbaldehydes with lipophilic substituents in both aromatic rings, which showed good anti-proliferative activities. The imine **B** (Fig. 1) strongly inhibited tubulin polymerization with an IC_{50} value of 1.2 μM, which was lower than that of colchicine (5 μM) in this assay [24].

On the other hand, thiosemicarbazones exhibit diverse biological activities, such as anti-plasmoid [5], anti-leishmanial [25], anti-microbial [26], anti-tumor [27, 28], and anti-oxidant [29] properties. Huang et al. synthesized another series of thiosemicarbazones, **C**, which exhibited a broad anti-proliferative activity in a panel of human tumor cells (Fig. 2). It blocked topoisomerase IIα-catalyzed ATP hydrolysis by competing with ATP for binding to the ATPase domain of topoisomerase IIα [30].

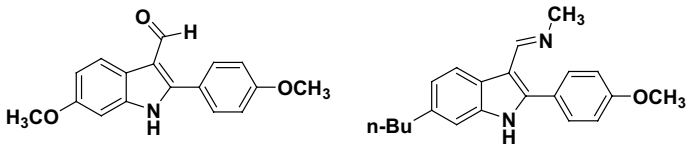

Fig. 1 Some potent anti-cancer 2-phenylindole-3-carbaldehyde analogs

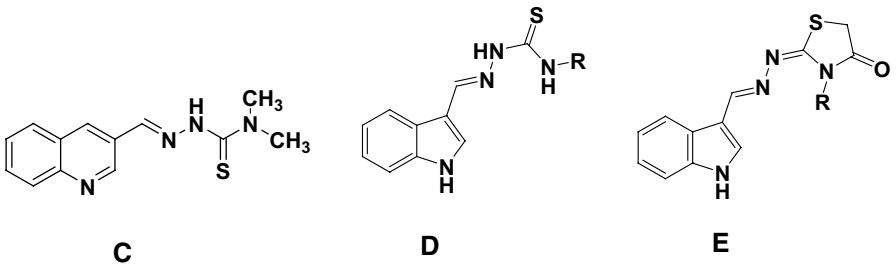

Fig. 2 Thiosemicarbazone derivative demonstrating profound anti-cancer activity

In 2017, de Oliveira et al. reported some thiosemicarbazone derivatives, as well as their in vitro antiproliferative activity against eight human tumor cell lines via inhibition of topoisomerase IIα (derivatives of **D** and **E**, Fig. 2) [4]. It has been revealed that a series of indole thiosemicarbazones, **D** derivatives, has been much more active than indole-thiazolidinone series (**E** derivatives). The molecular structures of **C** and **D** and **E** are provided in Fig. 2.

In order to find some novel multitarget indole anti-tumor and anti-oxidant agents, we focused on the design and synthesis of some novel chemical hybrids of indole and thiosemicarbazone pharmacophores. Different substituted aryl groups were incorporated into the structure to investigate the importance of substitutions at the C-2 position of the indole ring. Substitution of the thiosemicarbazone moiety with a methyl group have increased the antiproliferative activities against four human tumor cell lines [30]. Here, in search for the same effect, we substituted the thiosemicarbazone pharmacophore with a methyl group. Substituted phenyl ring was incorporated in this position as well. The general structure of the designed compounds is provided in Fig. 3.

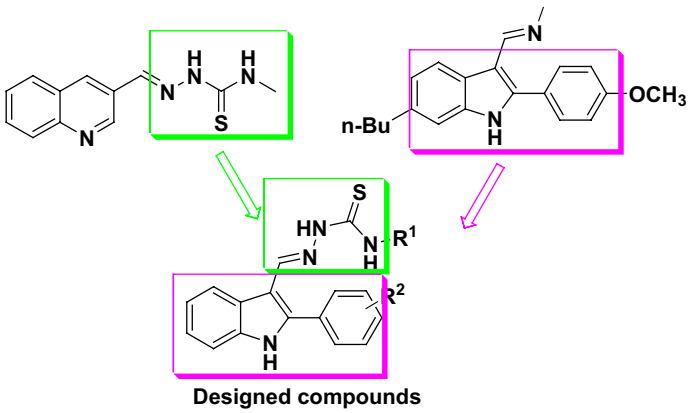

Fig. 3 General structure of the designed compounds

Results and discussion

Chemistry

The synthesis of thiosemicarbazone derivatives **(6a–p)** was performed in three steps as shown in Scheme 1. First, a nucleophilic addition reaction between hydrazine and isothiocyanates produced a thiosemicarbazide [30]. In another reaction, substituted indole 2-aryl was generated by Fischer reaction of substituted acetophenone and phenyl hydrazine [31]. Subsequently, the formyl group was introduced in position 3 of the indole by a Vilsmeier reaction with DMF and $POCl_3$ [25]. In the third step, the synthesized substituted indole 2-aryl 3-carboxaldehyde reacted with substituted thiosemicarbazide in the presence of a catalytic amount of CH_3COOH, via a condensation reaction, leading to thiosemicarbazone derivatives [32]. Crystallization of the products was performed in ethylacetate/petroleum ether, and the reaction yields ranged from 71 to 85%. Finally, the thiosemicarbazone structures (**6a–p**) were determined by ^1H and ^{13}CNMR, IR, ESI–MS and elemental analyses. The IR spectra of compounds **6n–p** display the expected absorption bands for NH at 3211–3441 cm^{-1}. In addition, these compounds show stretching of C=N and C=S bonds around 1593–1609 and 1196–1238 cm^{-1}, respectively. As exemplified by the ^1HNMR analysis of 1-((2-phenyl-1H-indol-3-yl)methylene)-4-p-tolylthiosemicarbazide (**6h**), the singlet at δ 2.90 corresponds to the *para*-methyl group at the phenyl ring. The phenyl protons substituted at 2-indole position appeared at 7.52, 7.59, and 7.66 ppm. Moreover, the *para*-methyl phenyl group at the thiosemicarbazone moiety

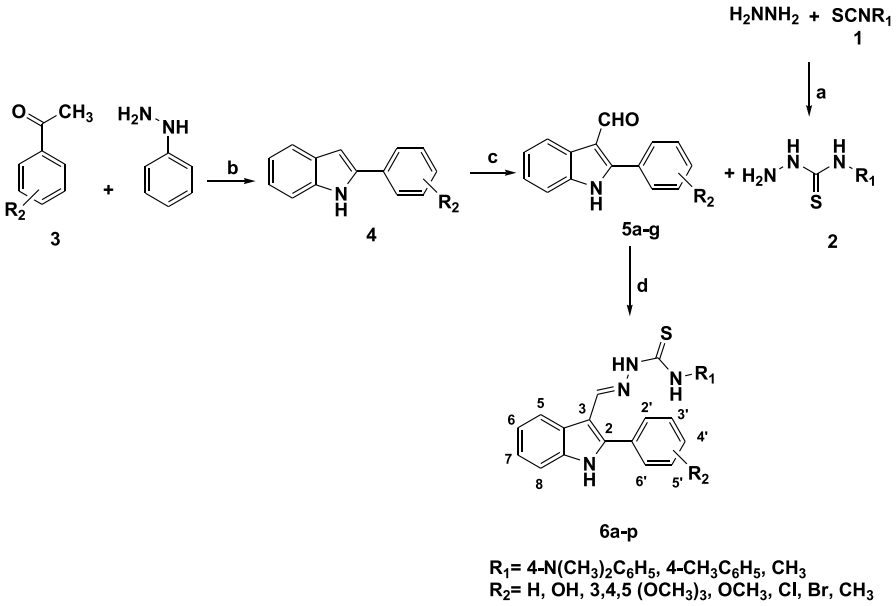

Scheme 1 Reagents and conditions: (a) *iso*propanol, 30 min; (b) (i) CH_3COOH, EtOH, reflux (ii) polyphosphoric acid, 120 °C; (c) $POCl_3$, DMF, 70 °C; (d) EtOH, CH_3COOH, reflux

displayed two doublets at 6.73 and 7.35 ppm. Also, the indole protons occurred as two triplets at 7.16 and 7.24 ppm and two doublets at 7.44 and 8.35 ppm. The singlet at 8.59 ppm related to imine proton (H–C=N) confirms the success of the reaction between *para*-tolyl thiosemicarbazide and 2-phenyl indole carbaldehyde. In addition, the signal related to N–H appeared at 9.31 ppm. The N–H connected to phenyl group (HN–Ph) showed a singlet at 11.42 ppm. Moreover, the N–H indole ring signal appeared at 11.94 ppm. Similarly, in the ^{13}CNMR spectra, the azo methane group (H–C=N) occurred at 141.5 ppm, while the C=S group appeared at 174.6 ppm. Also, the *E* configuration was confirmed by the 2D NMR NOESY spectrum of compound **6h**. In this respect, there was a spatial correlation between hydrogen of =N–NH at 11.42 ppm and azomethine (–CH=N–) at 9.31 ppm. These results suggest the E configuration, which corroborates the NOESY spectrum of E thiosemicarbazone presented in the literature [5, 33]. In addition, ESI–MS confirmed the identity of all the synthesized compounds.

Biology

Anti-proliferative activity

The prepared derivatives **6a–p** were classified into three categories based on the diverse groups substituted on thiosemicarbazone moiety and C-2 indole ring. Then their inhibitory activities were evaluated against the *MCF-7* (breast), *A-549* (lung), and *Hep-G2* (liver) cell lines as summarized in Table 1. Compound **6g** with 4-dimethylaminophenyl moiety substituted on thiosemicarbazone and 4-methylphenyl group at C-2 position of the indole ring, exhibited the highest inhibitory activity against *MCF-7* and *HepG2* with IC_{50} values of 23.39 µM and 24.46 µM, respectively. For etoposide as the reference drug IC_{50} values were = 34.25 µM against *MCF-7* and 33.17 µM against *HepG2*. In addition, compound **6n**, with the methyl group substituted on thiosemicarbazone and 4-methoxyphenyl substitute at C-2 position of the indole ring, revealed the highest inhibitory activity against *A-549* cell line with IC_{50} of 12.5 µM. This result also indicated that the methoxy group at *para* phenyl ring of indole C-2 position and methyl group substituted on thiosemicarbazone moiety had important roles in the inhibition activity of **6n** against *A-594* cell line. Remarkably, those compounds bearing 4-dimethylaminophenyl group substituted on the thiosemicarbazone moiety and substitutes of 4-hydroxylphenyl (**6b**) and 3,4,5-trimethoxyphenyl (**6c**) at C-2 position of the indole ring exhibited a high *MCF-7* inhibitory activity, compared with the other compounds. Replacement of 3,4,5 trimethoxy moieties (**6c**) with 4-OH group (**6b**), at C-2 position of the indole ring improved the activity (Table 1).

Moreover, compounds **6m–p** in the third class that have methyl group substituted to thiosemicarbazone moiety did not show any activity against *MCF-7* cell line ($IC_{50} > 100$ µM), whereas these compounds exhibited the highest cytotoxic activity against *A-549* and *Hep-G2* cell lines compared with others. This shows that the presence of small groups (e.g. methyl) at the thiosemicarbazone moiety is possibility significant for activity against both *A-549* and *Hep-G2* cell lines, a result that is

Table 1 Anti-cancer activity and calculation of cLogP and Goldscore fitness values for indole-thiosemicarbazone derivatives of **6**

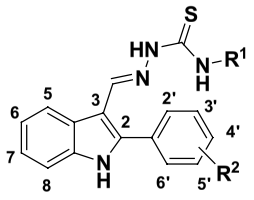

Compound	R1	R2	MCF-7[a]	A-549[a]	Hep-G2[a]	cLogP[b]	Goldscore fitness[c]	Goldscore fitness[d]
6a	4-N(Me)$_2$C$_6$H$_5$	H	> 100	> 100	> 100	5.24	61.04	53.97
6b	4-N(Me)$_2$C$_6$H$_5$	4-OH	31.38 ± 4.96	> 100	> 100	4.76	55.45	59.25
6c	4-N(Me)$_2$C$_6$H$_5$	3,4,5(OMe)$_3$	35.78 ± 6.89	> 100	> 100	4.87	48.93	55.89
6d	4-N(Me)$_2$C$_6$H$_5$	4-OMe	> 100	> 100	36.43 ± 4.73	5.30	59.48	62.64
6e	4-N(Me)$_2$C$_6$H$_5$	4-Cl	> 100	> 100	72.68 ± 6.45	5.92	61.42	56.82
6f	4-N(Me)$_2$C$_6$H$_5$	4-Br	> 100	> 100	> 100	6.05	51.78	48.92
6g	4-N(Me)$_2$C$_6$H$_5$	4-Me	23.39 ± 5.47	80.84 ± 7.5	24.46 ± 1.05	5.69	61.31	51.20
6h	4-MeC$_6$H$_5$	H	> 100	> 100	42.83 ± 5.54	5.59	62.41	62.55
6i	4-MeC$_6$H$_5$	4-OH	24.97 ± 5.32	> 100	> 100	5.11	63.97	61.54
6j	4-MeC$_6$H$_5$	4-OMe	> 100	> 100	> 100	5.64	63.97	68.27
6k	4-MeC$_6$H$_5$	4-Cl	> 100	> 100	> 100	6.27	62.35	63.62
6l	4-MeC$_6$H$_5$	4-Br	> 100	> 100	> 100	6.40	64.11	64.82
6m	Me	4-OH	> 100	24.20 ± 1.70	51.70 ± 4.10	3.60	49.02	59.61
6n	Me	4-OMe	> 100	12.50 ± 1.00	56.00 ± 6.30	4.14	52.70	59.61
6o	Me	4-Cl	> 100	22.95 ± 1.63	48.94 ± 3.91	4.76	53.07	54.76

Table 1 (continued)

Compound	R1	R2	MCF-7[a]	A-549[a]	Hep-G2[a]	cLogP[b]	Goldscore fitness[c]	Goldscore fitness[d]
6p	Me	4-Br	> 100	92.11 ± 6.33	49.97 ± 5.52	4.89	51.43	57.07
Etoposide	–	–	34.25 ± 3.12	38.23 ± 1.89	33.17 ± 3.19	0.7	–	–
Colchicine	–	–	7.10 ± 0.61	1.9 ± 0.23	6.0 ± 0.49	1.10	–	–

[a]The IC_{50} (half maximal inhibitory concentration) values represent an average of three independent experiments (mean ± SD)

[b]The logP value of a compound which is the logarithm of its partition coefficient between *n*-octanol and water log(coctanol/cwater) is a well established measure of the compound's hydrophilicity

[c]The binding affinity of ligand with tubulin

[d]The binding affinity of ligand with ATPase domain of topoisomerase II

in accordance with the literature [30]. In the second series (**6h–l**), compounds **6h** (IC_{50} = 42.83 μM against *Hep-G2*) and **6i** (IC_{50} = 24.97 μM against *MCF-7*) showed strong activities, whereas other compounds in the series were weak with IC_{50} values more than 100 μM. This modification revealed that the *para* hydroxylphenyl ring substituted at the C-2 position of indole ring was ideal for inhibitory activity against *MCF-7*. However, unsubstituted phenyl ring incorporated to the C-2 position of indole of **6h** is optimum for cytotoxic activity against *Hep-G2* cell line.

In the first series (**6a–g**), compounds **6d** showed good activity against *Hep-G2* cell line (IC_{50}s = 36.43 μM). Replacement of methoxy (**6d**) with chloro group (**6e**) in *para* position of the phenyl ring substituted at indole C-2 position led to a decrease in the cytotoxicity. Compounds **6a**, **6f**, **6j**, **6k**, and **6l** demonstrated no cytotoxicity against three cell lines (IC_{50} > 100).

Interestingly, the presence of methyl substituent on the phenyl ring at the C-2 position of indole ring increased the cytotoxicity of compound **6g** in the first series (**6a–g**) with IC_{50} values of 23.39 μM, 80.84 μM, and 24.46 μM against *MCF-7*, *A-594*, and *Hep-G2* cell lines, respectively. Compounds with other substituents in this position showed less activities. The presence of hydroxyl, methoxy, chloro and bromo groups on the *para* phenyl ring at the indole C-2 position of the second series compounds (**6i–l**) did not display any cytotoxic activity against *A-594* and *Hep-G2* cell lines (IC_{50} > 100). *Para* chloro and *para* bromophenyl substituents at indole C-2 position in the third group (compounds **6o** and **6p**), showed the highest activities against *Hep-G2* (IC_{50}s = 48.94 μM and 49.97 μM). The assay results revealed that probably the presence of halogens (Cl and Br) on *para* phenyl ring at C-2 position of indole increased the activity. However, incorporation of hydroxyl and methoxy substituents at the same position led to a much more reduction in cytotoxicity (IC_{50}s = 51.7 μM and 56.0 μM, respectively). Finally, it should be noted that compounds in the **6m–p** series showed a higher activity against *A-549* and *Hept-G2* compared with other series and that compounds in the **6a–g** series exhibited better activities against *MCF-7*.

Morphological evaluation by fluorescence microscopy

The most active compound **6n** was selected to determine the apoptotic or necrotic cell death in *A-549* cells morphologically by the acridine orange/ethidiumbromide (AO/EB) double staining test [34]. AO penetrates the living as well as the dead cells and emits green fluorescence as a result of intercalation into double-stranded DNA, while ethidium bromide (EB) staining precedes the loss of membrane integrity and intercalates in DNA of cells with an altered cell membrane and emits red fluorescence. The AO/EB staining that is sensitive to DNA was used to access changes in nuclear morphology. Analysis of the AO/EB staining revealed that the selected most potent compound, **6n**, clearly can be the inducer of apoptosis as the appearance of chromatin condensation and nuclear fragmentation are evident in Fig. 4. As shown, the viable cells are observed green, but the apoptotic cells with chromatin condensation or fragmentation show orange-stained nuclei. The lung cancer cell treated with the most potent test compound showed extended apoptosis relative to the control.

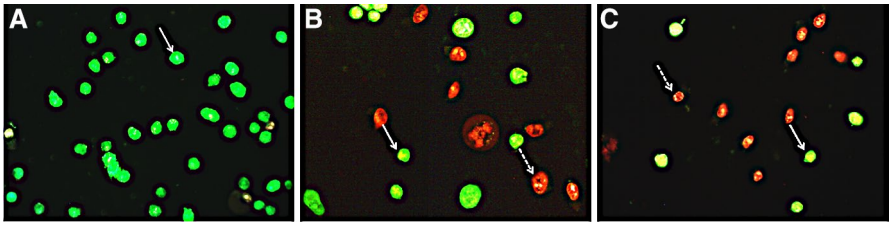

Fig. 4 AO/EB double staining of cancer cells with characteristic symptoms of apoptosis of *A-549* **a** DMSO 1% as control, **b**, **c** cells treated for 24 h with IC_{50} concentrations of etoposide and **6n**, respectively

Flow cytometry analysis of apoptotic cells with Annexin V-FITC/PI staining

Apoptosis induction of the prepared compounds was also confirmed by flow cytometry analysis. Annexin V-FITC/PI followed by flow cytometric analysis detects the externalization of phosphatidylserine in apoptotic cells using recombinant annexin V conjugated to green-fluorescent FITC dye and dead cells using propidium iodide (PI). The results indicated that the novel compounds induced apoptosis of *A-549* cancer cells. Flow cytometric analysis revealed that the cells underwent apoptosis after treatment with the test compounds. As illustrated in Fig. 5, the apoptotic index of compound **6n** was compared with the negative control and etoposide in *A-549* cells. Double staining followed by flow cytometric analysis revealed the percentage of apoptotic cells as 27.5% resulting from treatment with compound **6n** after a 24-h incubation. In addition, the corresponding value obtained after treatment with etoposide was 24.5% following a 24-h incubation (Fig. 5).

Anti-oxidant assay

All the synthesized compounds **6a–p** were subjected to in vitro 2,2-diphenyl-1-picrylhydrazyl (DPPH) assay in order to assess their radical scavenging properties. DPPH is a stable free radical with violet color. When a compound donates a radical

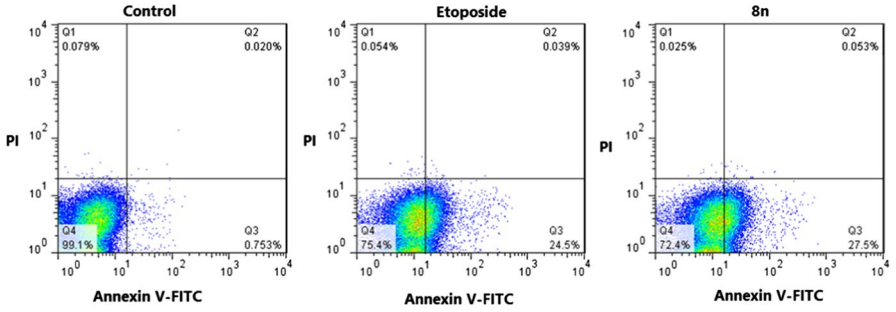

Fig. 5 Flow cytometric analysis of *A-549* cells treated with the prepared compound **6n**. Cells were stained with Annexin V-FITC/PI and quantitated by flowcytometry. Cells were treated with DMSO 1% (negative control) or with IC_{50} values of etoposide (positive control) and compound **6n**

Table 2 IC_{50} values for DPPH radical scavenging activity of indole–thiosemicarbazide derivatives **6**

Compound	DPPH IC_{50}^{a} (μM)	Compound	DPPH IC_{50}^{a} (μM)
6a	0.117 ± 0.01	**6j**	0.204 ± 0.008
6b	0.041 ± 0.003	**6k**	0.210 ± 0.02
6c	0.227 ± 0.05	**6l**	0.228 ± 0.03
6e	0.121 ± 0.007	**6m**	0.160 ± 0.005
6f	0.241 ± 0.01	**6n**	0.336 ± 0.04
6g	0.148 ± 0.006	**6o**	0.567 ± 0.01
6h	0.043 ± 0.001	**6p**	0.630 ± 0.05
6i	0.016 ± 0.001	**Ascorbic**	0.655 ± 0.02

[a]The IC_{50} values represent an average of three independent experiments (mean ± SD)

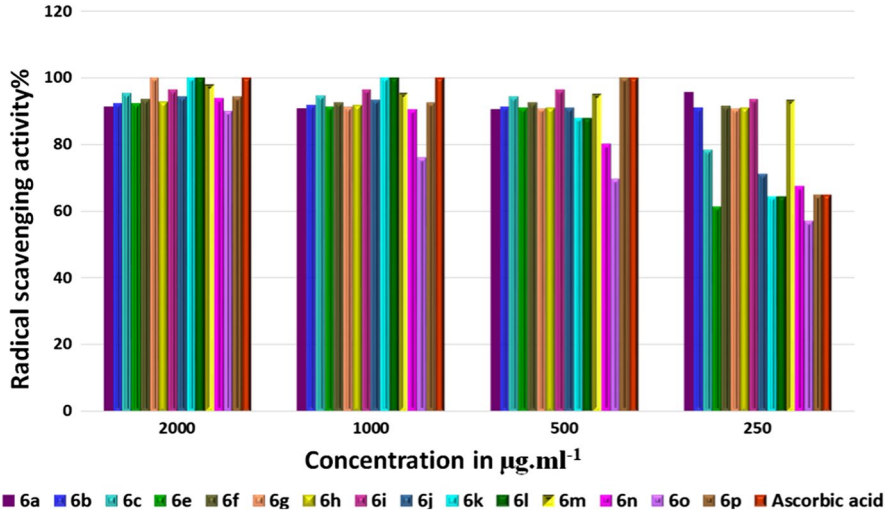

Fig. 6 DPPH radical scavenging activities of indole-thiosemicarbazone derivatives **6**

hydrogen species to a DPPH molecule, DPPH is decolorized, and thus the absorbance of DPPH is decreased. In brief, lighter violet color accounts for higher anti-oxidant activity. The ratio of anti-oxidant/DPPH required to decrease the concentration of DPPH to 50% of its initial value, is denoted as IC_{50} or is an indicator of the radical scavenging activity [35]. The anti-oxidant activities of the compounds were screened at the concentrations of 125–2000 μg mL^{-1} at 517 nm for the DPPH assay, and the obtained results are presented in Table 2 and Figs. 6 and 7. Ascorbic acid was used as the standard. Based on the experimental results, it was found that all compounds showed potent anti-oxidant activities in the range of 0.016–0.630 μM compared with ascorbic acid (0.655 μM). A higher anti-oxidant activity is reflected in a lower IC_{50} value.

In DPPH assay, antioxidants react with free radicals by single electron transfer (SET) mechanism. In SET mechanisms, the antioxidant provides an electron to the

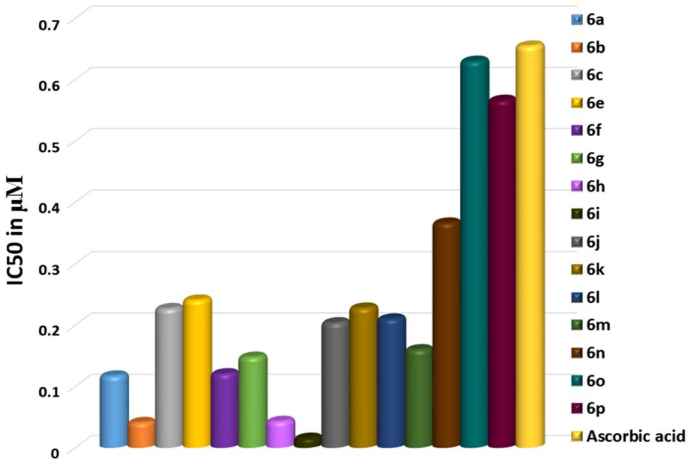

Fig. 7 IC_{50} for compounds (**6a–p**) using DPPH assay

free radical and itself then becomes a radical cation [36]. It seemed that existence of a good electron transfer group such as phenyl at thiosemicarbazide moiety, increases antioxidants activity. Thus, compounds **6a–g** and **6h–l** having 4-dimethylaminophenyl and 4-methylphenyl groups substituted to thiosemicarbazide revealed higher antioxidant activity than compounds **6m–p** having methyl group. Antioxidant activity studies displayed that bulky substitution on the phenyl ring incorporated on the indole C-2 position makes steric hindrance that avoids from near DPPH molecule, thus these compounds showed weak antioxidant activity compared with the unsubstituted compound. Therefore, compounds **6a** and **6h** displayed high antioxidant activity. Moreover, compounds **6b**, **6i** and **6m** having 4-hydroxyphenyl at C-2 indol ring exhibited good antioxidant activity because of OH group.

Molecular docking study

Molecular docking as an important method in structure-based computer-assisted drug design, predicts the main binding mode(s) of a ligand with a protein of known 3D structure [37]. Molecular docking simulations and analysis of the binding modes of the designed compounds within tubulin and ATPase domain of topoisomerase IIα binding active sites were performed by Gold 5.3.0 in order to rationalize the anticancer activity results. At first, the binding sites of ANP and colchicine were precisely characterized in the active sites of ATPase domain of topoisomerase IIα and tubulin, respectively. As presented in Fig. 8a, formation of hydrogen bonds between some parts of ANP and Gly166, Tyr165, Gly164, Asn163, Ser148, Ser149, Gln376, Asn150, Asn91, Lys168, Arg162, Ala167, and Asn120 residues was distinguished. In addition, hydrophobic interactions of ANP with Ile125, Ile141, Gly161, Asn95, Lys378 and Ala92 were fully recognized, as indicated which can also be observed in Fig. 8.

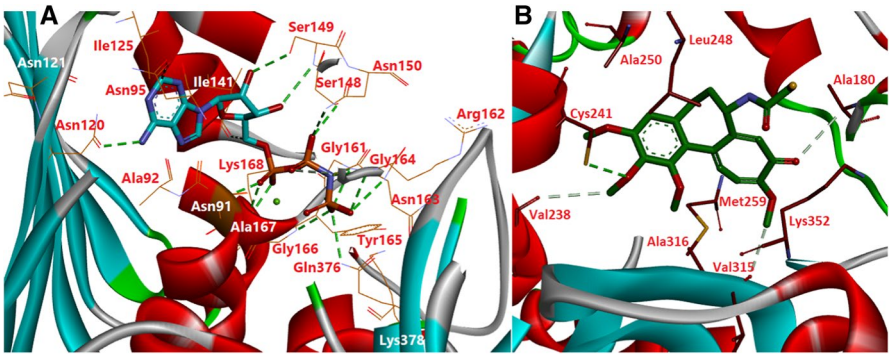

Fig. 8 Binding sites of **a** ANP and **b** colchicine in the active sites of ATPase domain of topoisomerase IIα and tubulin. Green dashed lines indicate hydrogen bonds

Figure 8b also clearly represents the hydrogen bond formation of methoxy group and Cys241 residue. Moreover, the hydrophobic interactions of different parts of colchicine with Ala316, Lys352, Val315, Met259, Ala180, Ala250, Val238, and Leu248 were well established.

Docking studies revealed that the binding modes of the most active compounds are coherent with co-crystallized colchicine and ANP. Compounds **6j** and **6l** showed the highest goldscore fitness values at the topoisomerase IIα and tubulin active sites (Table 1). It seems that *para* methyl phenyl substituted to the thiosemicarbazone moiety of **6j** and **6l** might be responsible for additional hydrophobic interactions with topoisomerase IIα and tubulin. These two compounds showed weak anti-cancer activities (Table 1). A lower anti-cancer activity might be attributed to the improper geometric orientation of compounds in the topoisomerase IIα and tubulin binding sites. This can be seen in Figs. 9 and 10 by superimposing **6j** and **6l** with ANP and colchicine in the active sites of both targets.

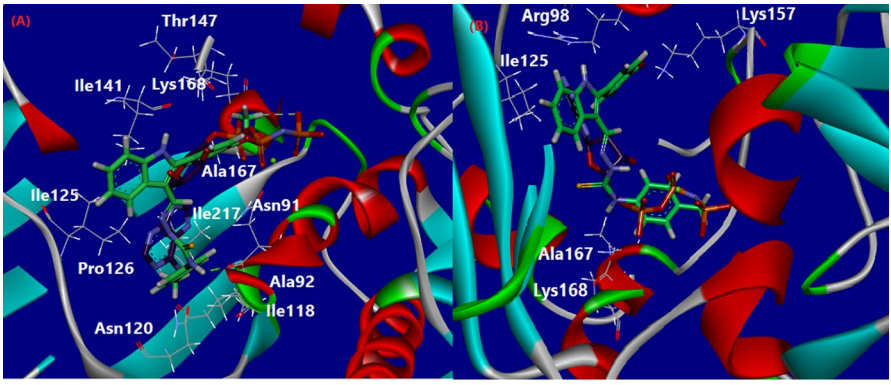

Fig. 9 Interactions of **6j** (**a**) and **6l** (**b**) in topoisomerase IIα active site and superimposition of both with ANP (dark blue)

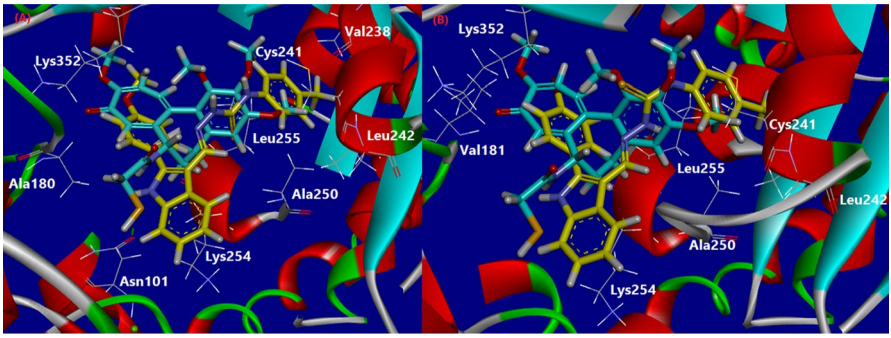

Fig. 10 Interactions of **6j** (**a**) and **6l** (**b**) in the tubulin active site and superimposition of both with colchicine (blue)

According to the cLogP data, **6l** and **6j** are lipophilic (Table 1). Thus, these compounds increase hydrophobic interactions in the hydrophobic pocket of both enzymes and show better goldscore fitness values. Compound **6n** was the most potent compound with IC_{50} equal to 12.5 µM against *A-549* cell line. Docking studies demonstrated that **6n** participated in the key interactions with the binding site residues of both targets (Goldscore fitness = 52.70 and 59.61 for tubulin and topoisomerase IIα, respectively). Detailed analysis of hydrophobic binding patterns in tubulin active site show that two interactions exist between indole ring of **6n** and Leu248 and Lys254 (Fig. 11a). Moreover, the methyl substituent of thiosemicarbazone is responsible for further hydrophobic interactions with Ala317 and Lys352 in the hydrophobic pocket. The methyl group of *para* methoxyphenyl substituent at the C-2 position of indole ring formed hydrophobic interactions with the Val315 and Met259 residues. In addition, analysis of the hydrophobic binding patterns in the

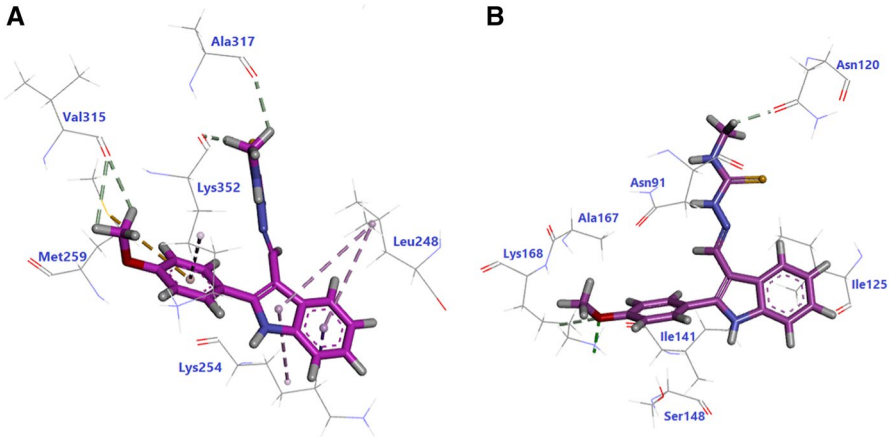

Fig. 11 Compound **6n** at active sites of tubulin (**a**) and topoisomerase IIα (**b**). Green dashed line indicates hydrogen bond

topoisomerase IIα active site revealed that the methyl group of thiosemicarbazone interacted with Asn120 (Fig. 11b). Thiosemicarbazone substituent at the C-3 indole ring formed a hydrophobic interaction with Asn91 amino acid. Other parts of the molecule had hydrophobic contacts with Ile141, Ser148, Ala167, and Lys168 residues in topoisomerase IIα hydrophobic packet. Furthermore, **6n** was able to form a hydrogen bond between the oxygen atom of the methoxy group and amino group of Lys168 residue. Thus, the existence of this hydrogen bond led to an increase in the affinity of **6n** to topoisomerase IIα (Goldscore fitness = 59.61) compared with tubulin (Goldscore fitness = 52.70).

Replacement of the methyl substituent of the thiosemicarbazone moiety in compound **6n** with *para* methylphenyl (**6j**) led to a weak activity against the *A-549* cell line, and the *para N,N*-dimethylphenyl analogue (**6d**) showed a good activity against the *Hep-G2* cell line. Docking results obtained for compound **6d** displayed more affinity to topoisomerase IIα than tubulin (Goldscore fitness = 59.48 and 62.64 for tubulin and topoisomerase IIα, respectively). In addition, reduction in lipophilic moieties (methyl vs. *N,N*-dimethylphenyl ring) at the thiosemicarbazone substituent increased the activity. Compound **6d** contributed in no hydrogen bond to the tubulin active site amino acids. This compound only formed hydrophobic interactions with the Leu242, Cys241, Ala354, Ala250, Lys254, Asn101, Leu255, Val318, Ala354, and Ala316 residues. Similar to tubulin, compound **6d** did not show any hydrogen bond with topoisomerase IIα active site amino acids. Furthermore, investigation of hydrophobic binding patterns showed that these interactions were formed between the *N,N*-dimethyl amino group at the *para* position of the phenyl ring and Thr215 and Asn120 residues. The phenyl ring of thiosemicarbazone interacted with Ile125. Also, other moieties of the molecule formed hydrophobic interactions with the Ser149, Ile141, Ser148, and Thr147 amino acids. Interactions of **6d** with the binding site amino acids of tubulin and topoisomerase IIα are shown in Fig. 12.

Replacement of the methoxy group at the *para* position of the phenyl ring of C-2 indole ring in **6d** with the methyl group in **6g** increased the activity against three cell lines. Based on the docking results, analogues with increased hydrophilic character were equal to or slightly improved in potency, but addition of polar groups had a negative effect. Thus, the 4-methylphenyl group provided additional hydrophobic contacts with residues at the active site. Moreover,

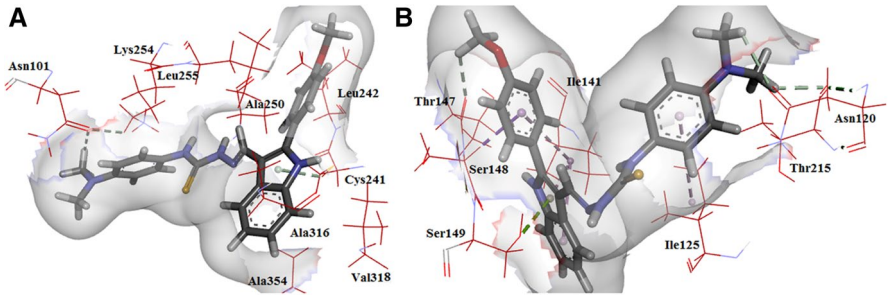

Fig. 12 Compound **6d** at active sites of tubulin (**a**) and topoisomerase IIα (**b**)

docking observations for compound **6g** showed that it had more affinity to tubulin than topoisomerase IIα (goldscore fitness = 61.31 vs. 51.20). The docking results revealed that compound **6g** formed hydrogen bond with Thr147 in the topoisomerase IIα active site, while compound **6g** did not participate in hydrogen bonding with the tubulin active site. Compound **6g** showed hydrophobic contacts with Ala354, Val318, Leu255, Lys254, Leu252, Ala250, Ala316, Cys241, and Leu242 tubulin residues and Ala167, Asn91, Lys157, Arg98, and Ile125 topoisomerase IIα amino acids. The hydrogen bond and hydrophobic interactions of **6g** in both proteins are shown in Fig. 13.

Substitution of 3,4,5-trimethoxyphenyl moiety at the *para* position of the phenyl ring of C-2 indole ring reduced the goldscore fitness values compared with *para* hydroxyphenyl and *para* chlorophenyl substitutions at the same position. Docking studies displayed that the presence of two methoxy groups in *meta* positions of **6c** caused steric hindrance that changed its position in the active site, thus the interactions of compound **6c** decreased with the nearby amino acids of both proteins.

Replacing *para* chlorophenyl (**6e**) with *para* hydroxyphenyl (**6b**) at the C-2 position of the indole ring decreased the goldscore fitness value in interaction with tubulin. According to the cLogP data, **6e** is more lipophilic than **6b** (cLogP = 5.92 vs. 4.76). This shows that the tubulin active site is lipophilic, and an extra lipophilic group (methyl vs. hydroxyl) increases hydrophobic contacts with lipophilic amino acids. Docking results of compounds **6h** and **6i** were the same in the two proteins (Table 1). The presence of a hydroxyl group or hydrogen atom at the *para* position of the phenyl ring substituted on the indole C-2 position is not important for the affinity. Finally, it was found that compound **6n** was the most potent compound against the *A-549* cell line, and compound **6g** was the most potent compound against all three cell lines. Compounds **6j** and **6l** showed the highest goldscore fitness values in molecular docking studies. In addition, compounds of the third series (**6m–p**) indicated higher activity than those in the other series. Based on the cLogP data, this series has the least cLogP values (3.60–4.89), thus this range of cLogP is suitable for the cytotoxicity activity against *A-549* and *Hep-G2* cell lines.

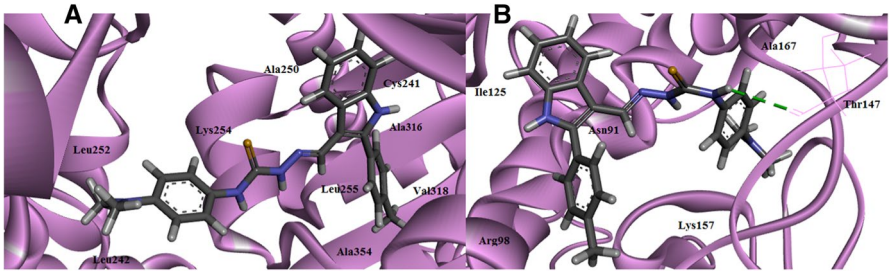

Fig. 13 Interactions of compound **6g** at active sites of tubulin (**a**) and topoisomerase IIα (**b**). Green dashed line indicates hydrogen bond

Conclusion

A new class of indole-thiosemicarbazons hybrids were designed, synthesized, and evaluated as cytotoxic agents against MCF-7, A-549, and Hep-G2 cell lines. Etoposide and colchicine were the reference drugs. The synthesized compounds were generally categorized into three classes based on the substituted groups at the thiosemicarbazone moiety, as well as C-2 position of the indole moiety. Compound **6n** revealed the highest inhibitory activity against *A-549* cell line. Moreover, compound **6g** displayed a high anti-proliferative activity with IC_{50} values between 23.39 and 80.84 μM against three studied cell lines. Interestingly, introduction of a methyl group at the thiosemicarbazone moiety **(6m–p)**, showed a higher activity against *A-549* and *Hep-G2* compared with other series. In addition, morphological analysis by the acridine orange/ethidium bromide double staining test and flow cytometry analysis confirmed induction of apoptosis in *A-549* cells by compound **6n**. Moreover, all of the compounds displayed excellent anti-oxidant activities in the range of 0.015-0.630 μM compared with ascorbic acid (0.655 μM). Compound **6h** bearing a methyl group on the *para* position of the phenyl thiosemicarbazone moiety and *para* hydroxyl phenyl at C-2 position of the indole ring exhibited a strong free radical scavenging ability compared with other compounds.

Experimental

Chemistry

All reagents and solvents used in this work were commercially available (from Merck Chemical) and were used without further purification. Melting points were determined on a Kofler hot-stage apparatus (Reichert, Vienna, Austria) and uncorrected. TLC was conducted on silica gel 250 μm, F254 plates. The IR and NMR spectra were recorded using a Nicolet Magna FTIR 550 spectrophotometer (potassium bromide disks) and Bruker 500 MHz NMR instruments, respectively. Chemical shifts were reported in parts per million (ppm, δ), down filled from tetramethylsilane coupling constant (J) values are presented in Hz and spin multiplicities are given as s (singlet), d (double), t (triplet) and m (multiplet). Elemental analyses were carried out by a CHN-Rapid Heraeus elemental analyzer. The results of elemental analyses (C, H, N) were within $\pm 0.4\%$ of the calculated values. The atoms numbering of the target compound used for ^{1}HNMR are shown in Scheme 1.

General method for synthesis of substituted thiosemicarbazides (2)

Isothiocyanate **1** (2 mmol) was added dropwise to a stirred solution of hydrazine hydrate (24 mmol, 80%) in 20 mL of isopropanol. Precipitate was formed immediately. Stirring was continued for 30 min. Then the mixture was filtered and the

precipitate was washed with isopropanol three times to give substituted thiosemicarbazids **2** [30].

General method for synthesis of substituted 2-phenyl-1H-indoles (4a–g)

Appropriate amounts of substituted acetophenone **3** (1 mmol) and phenyl hydrazine (1 mmol) were mixed in ethanol (20 mL), and a few drops of glacial acetic acid were added. The solution was heated under reflux at 80 °C for 1–2 h. The solvent was evaporated in vacuo to give a solid that was added to polyphosphoric acid (PPA) (30 mL), and the mixture was slowly heated to 120 °C and kept at this temperature for a few hours until the reaction was complete (TLC monitoring). The mixture was allowed to cool and then poured into cold water (50 mL). The acidic solution was neutralized by the slow addition of NaOH (1 M), and the solid precipitate of the crude product was collected. Purification by column chromatography (hexane/ethyl acetate) gave the substituted 2-aryl indoles **4a–g** [31].

General procedure for synthesis of 2-arylindole-3-carbaldehydes (5a–g)

Under nitrogen gas, phosphorous oxychloride (10 mmol) was added dropwise to dry dimethylformamide (DMF) (10 mmol) while cooling in an ice bath, and the reaction mixture was stirred for 1 h. A solution of compound **4** (1 mmol) in DMF (50 ml) was added dropwise to the mixture with continuous stirring, which was then heated to 70 °C. The mixture was poured onto ice cold water (200 mL), naturalized with 40% NaOH, and extracted with chloroform. The chloroform extract was washed with water and dried over Na_2SO_4. The solvent was removed under vacuum. The residue was crystalized from an ethanol/water mixed solvent system [24].

2-phenyl-1H-indole-3-carbaldehyde (5a) Cream powder; Mp: 249–250 °C; Yield: 89%; ^{1}H NMR (500 MHz, DMSO-d_6, 25 °C, TMS) (δ, ppm): 7.24 (t, J = 7.9 Hz, 1H, H_6), 7.29 (t, J = 7.9 Hz, 1H, H_7), 7.51 (d, J = 7.9 Hz, 1H, H_8), 7.56–7.62 (m, 3H, $H_{3',5',4'}$), 7.78 (d, J = 9.3 Hz, 2H, $H_{2',6'}$), 8.21 (d, J = 7.9 Hz, 1H, H_5), 9.96 (s, 1H, CHO), 12.40 (s, 1H, NH-indole). ^{13}C NMR (125 MHz, DMSO-d_6): (δ, ppm) 112.1, 113.5, 121.2, 122.5, 123.7, 125.8, 128.9, 129.2, 129.8, 130.1, 135.9, 149.1, 185.5. Anal. Calcd. for $C_{15}H_{11}NO$: C, 81.43; H, 5.01; N, 6.33. Found: C, 81.53; H, 4.85; N, 6.45; IR (KBr, cm^{-1}): 3144 (N–H stretching), 3058 (Aromatic C–H stretching) 2858 (H–CO), 1625 (C=O), 1455 (C=C); ESI–MS (m/z): 222 $[M+H]^+$.

2-(4-hydroxyphenyl)-1H-indole-3-carbaldehyde (5b) Cream powder; Mp: 225–227 °C; Yield: 92%; ^{1}H NMR (500 MHz, DMSO-d_6, 25 °C, TMS) (δ, ppm): 6.97 (d, J = 7.6 Hz, 2H, $H_{3',5'}$), 7.19–7.26 (m, 2H, $H_{5,6}$), 7.45 (d, J = 7.5 Hz, 1H, H_7), 7.60 (d, J = 7.6 Hz, 2H, $H_{2',6'}$), 8.17 (d, J = 7.5 Hz, 1H, H_8), 9.92 (s, 1H, CHO), 10.04 (s, 1H, OH), 12.20 (s, 1H, NH-indole). ^{13}C NMR (125 MHz, DMSO-d_6): (δ, ppm) 111.6, 112.7, 115.8, 120.4, 120.9, 122.2, 123.3, 125.9, 131.2, 135.8, 149.8, 159.1, 185.5. Anal. Calcd. for $C_{15}H_{11}NO_2$: C, 75.94; H, 4.67; N, 5.93. Found: C, 76.04; H, 4.71; N, 5.72; IR (KBr, cm^{-1}): 3211 (N–H stretching), 3151 (OH), 3074 (Aromatic C–H

stretching), 2862 (H–CO), 1619 (C=O), 1455 (C=C), 1177 (C–O); ESI–MS (*m*/*z*): 238 $[M+H]^+$.

2-(3,4,5-trimethoxyphenyl)-1H-indole-3-carbaldehyde (5c) Cream powder, Mp: 191–194 °C; Yield: 83%; ^{1}H NMR (500 MHz, DMSO-d_6, 25 °C, TMS) (δ, ppm): 3.81 (s, 3H, OCH_3), 3.95 (s, 3H, OCH_3), 4.01 (s, 3H, OCH_3), 6.83 (d, $J=9.5$ Hz, 1H, $H_{2'}$), 7.23 (t, $J=7.9$ Hz, 1H, H_5), 7.30 (t, $J=7.9$ Hz, 1H, H_6), 7.43 (d, $J=9.5$ Hz, 1H, $H_{6'}$), 7.62 (d, J=7.9 Hz, 1H, H_7), 7.71 (s, 1H, CHO), 8.14 (d, $J=7.9$ Hz, 1H, H_8), 10.49 (s, 1H, NH-indole). ^{13}C NMR (125 MHz, DMSO-d_6): (δ, ppm) 54.4, 55.3, 105.0, 105.6, 110.1, 121.8, 122.4, 123.9, 126.0, 127.5, 135.9, 141.8, 151.4, 155.2, 185.4. Anal. Calcd. for $C_{18}H_{17}NO_4$: C, 69.44; H, 5.50; N, 4.50. Found: C, 69.65; H, 5.61; N, 4.59; IR (KBr, cm^{-1}): 3200 (N–H stretching), 3057 (Aromatic C–H stretching), 2844 (H–CO), 1617 (C=O), 1473 (C=C), 1120 (C–O); ESI–MS (*m*/*z*): 312 $[M+H]^+$.

2-(4-methoxyphenyl)-1H-indole-3-carbaldehyde (5d) Cream powder, Mp: 207–209 °C; Yield: 90%; ^{1}H NMR (500 MHz, DMSO-d_6, 25 °C, TMS) (δ, ppm): 3.87 (s, 3H, OCH_3), 7.16 (d, $J=8.7$ Hz, 2H, $H_{3',5'}$), 7.20–7.28 (m, 2H, $H_{5,6}$), 7.47 (d, $J=7.6$ Hz, 1H, H_7), 7.72 (d, $J=8.7$ Hz, 2H, $H_{2',6'}$), 8.18 (d, $J=7.6$ Hz, 1H, H_8), 9.94 (s, 1H, CHO), 12.28 (s, 1H, NH-indole). ^{13}C NMR (125 MHZ, DMSO-d_6): (δ, ppm) 55.8, 111.8, 113.2, 114.7, 120.9, 122.0, 122.4, 123.7, 125.9, 131.4, 135.9, 149.3, 160.6, 185.4. Anal. Calcd. for $C_{16}H_{13}NO_2$: C, 76.48; H, 5.21; N, 5.57. Found: C, 76.60; H, 5.29; N, 5.48; IR (KBr, cm^{-1}): 3147 (N–H stretching), 3056 (Aromatic C–H stretching), 2837 (H–CO), 1621 (C=O), 1454 (C=C), 1179 (C–O); ESI–MS (*m*/*z*): 252 $[M+H]^+$.

2-(4-chlorophenyl)-1H-indole-3-carbaldehyde (5e) Cream Powder, Mp > 50 °C; Yield: 93%. ^{1}H NMR (500 MHz, DMSO-d_6, 25 °C, TMS) (δ, ppm): 7.25 (t, $J=7.6$ Hz, 1H, H_6), 7.30 (t, $J=7.6$ Hz, 1H, H_7), 7.51 (d, $J=7.6$ Hz, 1H, H_8), 7.74 (d, $J=8.1$ Hz, 2H, $H_{3',5'}$), 7.80 (d, $J=8.1$ Hz, 2H, $H_{2',6'}$), 8.21 (d, $J=7.6$ Hz, 1H, H_5), 9.95 (s, 1H, CHO), 12.46 (s, 1H, NH-indole). ^{13}C NMR (125 MHZ, DMSO-d_6): (δ, ppm) 112.1, 113.6, 121.1, 122.6, 123.5, 123.9, 125.8, 129.0, 131.8, 132.0, 135.9, 147.4, 185.4. Anal. Calcd. for $C_{15}H_{10}ClNO$: C, 70.46; H, 3.94; N, 5.48. Found: C, 70.69; H, 3.85; N, 5.51; IR (KBr, cm^{-1}): 3168 (N–H stretching), 3036 (Aromatic C–H stretching) 2866, 1625, 1450; ESI–MS (*m*/*z*): 256 $[M+H]^+$.

2-(4-bromophenyl)-1H-indole-3-carbaldehyde (5f) Cream powder, Mp> 250 °C; Yield: 92%. ^{1}H NMR (500 MHz, DMSO-d_6, 25 °C, TMS) (δ, ppm): 7.25 (t, $J=7.6$ Hz, 1H, H_6), 7.30 (t, $J=7.6$ Hz, 1H, H_7), 7.51 (d, $J=7.6$ Hz, 1H, H_8), 7.74 (d, $J=8.3$ Hz, 2H, $H_{3',5'}$), 7.80 (d, $J=8.3$ Hz, 2H, $H_{2',6'}$), 8.20 (d, $J=7.6$ Hz, 1H, H_5), 9.95 (s, 1H, CHO), 12.47 (s, 1H, NH-indole). ^{13}C NMR (125 MHZ, DMSO-d_6): (δ, ppm) 112.1, 113.6, 121.1, 122.6, 123.5, 123.9, 125.5, 128.8, 131.9, 132.0, 136.2, 147.4, 185.2. Anal. Calcd. for $C_{15}H_{10}BrNO$: C, 60.02; H, 3.36; N, 4.67. Found: C, 60.21; H, 3.48; N, 4.60; IR (KBr, cm^{-1}): 3167 (N–H stretching), 3058 (Aromatic

C–H stretching), 2840 (H–CO), 1623 (C=O), 1452 (C=C); ESI–MS (*m*/*z*): 300 $[M+H]^+$.

2-p-tolyl-1H-indole-3-carbaldehyde (5g) Cream powder, Mp: 239–241 °C, Yield: 88%. ^{1}H NMR (500 MHz, DMSO-d_6, 25 °C, TMS) (δ, ppm): 2.41 (s, 3H, CH_3), 7.23 (t, $J=7.5$ Hz, 1H, H_6), 7.28 (t, $J=7.5$ Hz, 1H, H_7), 7.41 (d, $J=7.9$ Hz, 2H, $H_{3',5'}$), 7.49 (d, $J=7.5$ Hz, 1H, H_8), 7.67 (d, $J=7.9$ Hz, 2H, $H_{2',6'}$), 8.19 (d, $J=7.5$ Hz, 1H, H_5), 9.95 (s, 1H, CHO), 12.34 (s, 1H, NH-indole). ^{13}C NMR (125 MHz, DMSO-d_6): (δ, ppm) 21.0, 112.0, 113.3, 121.1, 122.4, 123.6, 125.8, 126.9, 129.6, 129.9, 135.9, 139.7, 149.1, 184.9. Anal. Calcd. for $C_{16}H_{13}NO$: C, 81.68; H, 5.57; N, 5.97. Found: C, 81.78; H, 5.48; N, 5.79; IR (KBr, cm^{-1}): 3213 (N–H stretching), 3061 (Aromatic C–H stretching), 2863 (H–CO), 1625 (C=O), 1452 (C=C); ESI–MS (*m*/*z*): 236 $[M+H]^+$.

General procedure for synthesis of compounds (6a–p)

The substituted 2-arylindole-3-carbaldehyde derivative **5a–g** (1 mmol) and a few drops of acetic acid were added to a solution of substituted thiosemicarbazide derivative **2** (1.2 mmol) in ethanol (10 mL) . The mixture was stirred at reflux for 1–3 h and then cooled to room temperature. Then the solid separated was filtered and recrystallized from the mixture of ethyl acetate and *n*-hexane to give compounds **6a–p** [32].

(E)-4-(4-(dimethylamino)phenyl)-1-((2-phenyl-1H-indol-3-yl)methylene)thiosemicarbazide (6a) Yellow to green powder; Mp: 210–212 °C; Yield: 75%; ^{1}H NMR (500 MHz, DMSO-d_6, 25 °C, TMS) (δ, ppm): 2.90 (s, 6H; NCH_3); 6.73 (d, $J=8.2$ Hz; $H_{2'',6''}$), 7.17 (t, $J=7.4$ Hz, 1H; H_6), 7.24 (t, $J=7.4$ Hz, 1H; H_7), 7.35 (d, $J=8.2$ Hz, 2H; $H_{3'',5''}$), 7.44 (d, $J=7.4$ Hz, 1H; H_8), 7.52 (t, $J=7.0$ Hz, 1H; $H_{4'}$), 7.59 (t, $J=7.0$ Hz, 2H; $H_{3',5'}$), 7.66 (d, $J=7.0$ Hz, 2H; $H_{2',6'}$), 8.34 (d, $J=7.4$ Hz, 1H; H_5), 8.57 (s, 1H; H–C=N), 9.29 (s, 1H; NH–Ph), 11.40 (s, 1H; NH–C=S), 11.92 (s, 1H; NH-indole); ^{13}C NMR (DMSO-d_6, 25 °C, TMS) (δ, ppm): 40.5, 107.4, 111.5, 112.0, 121.1, 122.6, 123.2, 125.2, 126.6, 128.6, 128.9, 129.0, 129.3, 130.9, 136.5, 141.5, 142.5, 148.4, 174.8; IR (KBr, cm^{-1}): 3305, 3211 (N–H stretching), 3136 (Aromatic C–H stretching), 1607 (C=N), 1536 (C=C), 1273 (C–N), 1199 (C=S); Anal. Calcd. for $C_{24}H_{23}N_5S$: C 69.71, H 5.61,N 16.94, Found: C 69.51, H 5.49, N 17.06; ESI–MS (*m*/*z*): 414 $[M+H]^+$.

(*E*)-4-(4-(dimethylamino)phenyl)-1-((2-(4-hydroxyphenyl)-1H-indol-3-yl) methylene) thiosemicarbazide (6b) Yellow powder; Mp: 220–221 °C; Yield: 81%; ^{1}H NMR (500 MHz, DMSO-d_6, 25 °C, TMS) (δ, ppm): 2.89 (s, 6H; NCH_3), 6.72 (d, $J=8.0$ Hz, 2H; $H_{3'',5''}$), 6.96 (d, $J=8.0$ Hz, 2H; $H_{3',5'}$), 7.13 (t, $J=7.6$ Hz, 1H; H_6), 7.19 (t, $J=7.6$ Hz, 1H; H_7), 7.36 (d, $J=8.0$, 2H; $H_{2'',6''}$), 7.40 (d, $J=7.6$ Hz, 1H; H_8), 7.48 (d, $J=8.0$ Hz, 2H; $H_{2',6'}$), 8.29 (d, $J=7.6$ Hz, 1H; H_5), 8.52 (s, 1H; H–C=N), 9.26 (s, 1H; NH–Ph), 9.88 (s, 1H; OH), 11.35 (s, 1H; NH–C=S), 11.74 (s, 1H, NH-indole); ^{13}C NMR (DMSO-d_6, 25 °C, TMS) (δ, ppm): 40.4, 106.4, 112,

115.7, 120.9, 121.6, 122.6, 122.6, 125.3, 126.3, 126.4, 128.6, 130.4, 130.7, 136.3, 141.8, 143.2, 148.3, 158.2, 174.6; IR (KBr, cm^{-1}): 3425, 3312 (N–H stretching), 3243 (OH), 3136 (Aromatic C–H stretching), 1608 (C=N), 1536 (C=C), 1271 (C–N), 1204 (C=S), 1177 (C–O); Anal. Calcd. for $C_{24}H_{23}N_5OS$: C 67.11, H 5.40, N 16.30, Found: C 67.24, H 5.45, N 16.25; ESI–MS (*m*/*z*): 430 $[M+H]^+$.

(E)-4-(4-(dimethylamino)phenyl)-1-((2-(3,4,5-trimethoxyphenyl)-1H-indol-3-yl) methylene) thiosemicarbazide (6c) Light yellow powder; Mp: 205–207 °C; Yield: 71%; ^{1}H NMR (500 MHz, DMSO-d_6, 25 °C, TMS) (δ, ppm): 2.91 (s, 6H; NCH_3); 3.81 (s, 3H; OCH_3), 3.95 (s, 3H; OCH_3), 3.98 (s, 3H; OCH_3), 6.73 (d, $J=8.7$ Hz, 2H; $H_{3',5'}$), 6.94 (s, 1H; $H_{2'}$), 7.17 (d, $J=7.5$ Hz, 1H; H_6), 7.27–7.37 (m, 4H; $H_{7,\ 2'',6''}$), 7.37 (s, 1H; $H_{6'}$), 7.47 (d, $J=7.8$ Hz, 1H; H_8), 8.36 (d, $J=7.8$ Hz, 1H; H_5), 8.92 (s, 1H; H–C=N), 9.49 (s, 1H; NH–Ph), 11.80 (s, 1H; NH–C=S), 11.89 (s, 1H; NH-indole); ^{13}C NMR (DMSO-d_6, 25 °C, TMS) (δ, ppm): 40.7, 54.7, 55.3, 107.1, 111.3, 114.4, 122.1, 122.4, 124.2, 125.2, 125.4, 127.2, 127.7, 128.6, 129.0, 130.7, 133.0, 142.5, 143.2, 153.5, 174.3; IR (KBr, cm^{-1}): 3441, 3312 (N–H stretching), 3144 (Aromatic C–H stretching), 1609 (C=N), 1533 (C=C), 1267 (C–N), 1196 (C=S), 1119 (C–O); Anal. Calcd. for $C_{27}H_{29}N_5O_3S$: C 64.39, H 5.80, N 13.91, Found: C 64.46, H 5.89, N 14.03; ESI–MS (*m*/*z*): 504 $[M+H]^+$.

(E)-4-(4-(dimethylamino)phenyl)-1-((2-(4-methoxyphenyl)-1H-indol-3yl) methylene) thiosemicarbazide (6d) Dark cream powder; Mp: 211–212 °C; Yield: 81%; ^{1}H NMR (500 MHz, DMSO-d_6, 25 °C, TMS) (δ, ppm): 2.90 (s, 6H; NCH_3), 3.85 (s, 3H; OCH_3), 6.73 (d, $J=7.7$, 2H; $H_{3'',5''}$), 7.14–7.22 (m, 4H; $H_{3',5',6,7}$), 7.36 (d, $J=7.7$ Hz, 2H; $H_{2'',6''}$), 7.42 (d, $J=7.2$ Hz, 1H; H_8), 7.60 (d, $J=7.2$ Hz, 2H, $H_{2',6'}$), 8.31 (d, $J=7.2$ Hz, 1H, H_5); 8.54 (s, 1H, H–C=N), 9.27 (s, 1H, NH–Ph), 11.38 (s, 1H; NH–C=S), 11.82 (s, 1H; NH-indole); ^{13}C NMR (DMSO-d_6, 25 °C, TMS) (δ, ppm): 40.4, 55.3, 106.7, 112, 114.3, 114.4, 121.0, 122.8, 123.2, 125.2, 126.3, 126.4, 128.5, 130.6, 136.3, 141.7, 142.6, 148.4, 159.8, 174.7; IR (KBr, cm^{-1}): 3307, 3239 (N–H stretching), 3147 (Aromatic C–H stretching), 1607 (C=N), 1531 (C=C), 1278 (C–N), 1205 (C=S), 1181 (C–O); Anal. Calcd. for $C_{25}H_{25}N_5OS$: C 67.69, H 5.68, N 15.79, Found: C 67.80, H 5.74, N, 15.86; ESI–MS (*m*/*z*): 444 $[M+H]^+$.

(*E*)-1-((2-(4-chlorophenyl)-1H-indol-3-yl)methylene)-4-(4-(dimethylamino) phenyl) thiosemicarbazide (6e) Yellow powder; Mp: 230–231 °C; Yield: 85%; ^{1}H NMR (500 MHz, DMSO-d_6, 25 °C, TMS) (δ, ppm): 2.89 (s, 6H, NCH_3), 6.72 (d, $J=8.0$ Hz, 2H; $H_{3'',5''}$), 7.17 (t, $J=7.6$, 1H; H_6), 7.24 (t, $J=7.6$ Hz, 1H; H_7), 7.34 (d, $J=8.0$ Hz, 2H; $H_{2'',6''}$), 7.44 (d, $J=7.6$ Hz, 1H; H_8), 7.60 (d, $J=8.0$ Hz, 2H; $H_{3',5'}$), 7.78 (d, $J=8.0$, 2H; $H_{2',6'}$), 8.34 (d, $J=7.6$ Hz, 1H; H_5), 8.52 (s, 1H; H–C=N), 9.30 (s, 1H; NH–Ph), 11.35 (s, 1H; NH–C=S), 11.98 (s, 1H; NH-indole); ^{13}C NMR (DMSO-d_6, 25 °C, TMS) (δ, ppm): 40.8, 107.9, 111.6, 112.2, 121.2, 122.3, 122.7, 123.5, 125.0, 125.8, 126.7, 129.4, 130.1, 131.3, 131.9, 136.5, 141.0, 141.1, 174.8; IR (KBr, cm^{-1}): 3310, 3211 (N–H stretching), 3148 (Aromatic C–H), 1608 (C=N), 1538 (C=C), 1273 (C–N), 1200 (C=S); Anal. Calcd. for $C_{24}H_{22}ClN_5S$: C 64.35, H 4.95, N 15.63, Found: C 64.24, H 4.87, N 15.55; ESI–MS (*m*/*z*): 448 $[M+H]^+$.

(*E*)-1-((2-(4-bromophenyl)-1H-indol-3-yl)methylene)-4-(4-(dimethylamino)phenyl) thiosemicarbazide (6f) Dark cream powder; Mp: 228–229 °C; Yield: 85%; ^{1}H NMR (500 MHz, DMSO-d_6, 25 °C, TMS) (δ, ppm): 2.87 (s, 6H, NCH_3), 6.72 (d, $J=8.7$ Hz, 2H; $H_{3'',5''}$), 7.16 (t, $J=7.7$, 1H; H_6), 7.24 (t, $J=7.7$ Hz, 1H; H_7), 7.34 (d, $J=8.7$ Hz, 2H; $H_{2'',6''}$), 7.44 (d, $J=7.7$ Hz, 1H; H_8), 7.60 (d, $J=8.3$ Hz, 2H; $H_{3',5'}$), 7.78 (d, $J=8.3$ Hz, 2H; $H_{2',6'}$), 8.36 (d, $J=7.7$ Hz, 1H; H_5), 8.53 (s, 1H; H–C=N), 9.32 (s, 1H; NH–Ph), 11.39 (s, 1H; NH–C=S), 12.00 (s, 1H, NH-indole); ^{13}C NMR (DMSO-d_6, 25 °C, TMS) (δ, ppm): 40.8, 107.9, 111.6, 112.6, 121.2, 122.3, 122.7, 123.4, 125.1, 126.6, 128.10, 130.1, 131.3, 131.9, 134.7, 136.6, 141.0, 141.12, 174.8; IR (KBr, cm^{-1}): 3325, 3246 (N–H stretching), 3173 (Aromatic C–H), 1609 (C=N), 1534 (C=C), 1275 (C–N), 1205 (C=S); Anal. Calcd. for $C_{24}H_{22}BrN_5S$: C 58.54, H 4.50, N 14.22, Found: C 58.68, H 4.57, N 14.27; ESI–MS (*m*/*z*): 494 $[M+H]^+$.

(*E*)-4-(4-(dimethylamino)phenyl)-1-((2-p-tolyl-1H-indo l-3-yl)methylene) thiosemicarbazide (6g) Yellow powder; Mp: 225–227 °C; Yield: 75%; ^{1}H NMR (500 MHz, DMSO-d_6, 25 °C, TMS) (δ, ppm): 2.41 (s, 3H; CH_3), 2.90 (s, 6H; NCH_3), 6.73 (d, $J=8.2$ Hz, 2H; $H_{3'',5''}$), 7.15 (t, $J=7.5$ Hz, 1H; H_6), 7.22 (t, $J=7.5$ Hz, 1H; H_7), 7.35 (d, $J=8.2$ Hz, 2H; $H_{2'',6''}$), 7.39 (d, $J=7.5$ Hz, 2H; $H_{3',5'}$), 7.43 (d, $J=7.5$ Hz, 1H; H_8), 7.55 (d, $J=7.5$ Hz, 2H; $H_{2',6'}$), 8.32 (d, $J=7.5$, 2H; H_5), 8.55 (s, 1H; H–C=N), 9.28 (s, 1H; NH–Ph), 11.38 (s, 1H; NH–C=S), 11.86 (s, 1H; NH-indole); ^{13}C NMR (DMSO-d_6, 25 °C, TMS) (δ, ppm): 31.2, 40.6, 107.2, 111.2, 111.5, 121.0, 122.5, 123.0, 125.2, 126.7, 127.0, 127.7, 128.1, 129.2, 129.6, 136.4, 138.5, 141.9, 142.8, 174.5; IR (KBr, cm^{-1}): 3310, 3212 (N–H stretching), 3132 (Aromatic C–H), 1607 (C=N), 1539 (C=C), 1272 (C–N), 1200 (C=S); Anal. Calcd. for $C_{23}H_{20}N_4S$: C 71.85, H 5.24, N 14.57, Found: C 71.96, H 5.30, N 14.66; ESI–MS (*m*/*z*): 428 $[M+H]^+$.

(*E*)-1-((2-phenyl-1H-indol-3-yl)methylene)-4-p-tolylthiosemicarbazide (6h) Yellow to green powder; Mp: 225–227 °C; Yield: 81%; ^{1}H NMR (500 MHz, DMSO-d_6, 25 °C, TMS) (δ, ppm): 2.90 (s, 3H; CH_3), 6.73 (d, $J=8.5$ Hz, 2H; $H_{3'',5''}$), 7.16 (t, $J=7.7$ Hz, 1H; H_6), 7.24 (t, $J=7.7$ Hz, 1H; H_7), 7.35 (d, $J=8.5$ Hz, 2H; $H_{2'',6''}$), 7.44 (d, $J=7.7$ Hz, 1H; H_8), 7.52 (t, $J=7.5$ Hz, 1H; $H_{4'}$), 7.59 (t, $J=7.5$ Hz, 2H; $H_{3',5'}$), 7.66 (d, $J=7.5$ Hz, 2H; $H_{2',6'}$), 8.35 (d, $J=7.7$ Hz, 1H; H_5), 8.59 (s, 1H; H–C=N), 9.31 (s, 1H; NH–Ph), 11.42 (s, 1H; NH–C=S), 11.94 (s, 1H; NH-indole); ^{13}C NMR (DMSO-d_6, 25 °C, TMS) (δ, ppm): 21.0, 108.8, 110.5, 121.6, 122.1, 123.3, 124.0, 125.1, 125.8, 126.3, 127.9, 130.0, 131.9, 134.2, 136.1, 136.9, 141.2, 141.5, 174.6; IR (KBr, cm^{-1}): 3310, 3209 (N–H stretching), 3159 (Aromatic C–H), 1607 (C=N), 1537 (C=C), 1273 (C–N), 1202 (C=S). $C_{23}H_{20}N_4S$: C 71.85, H 5.24, N 14.57, Found: C 71.65, H 5.19, N 14.60; ESI–MS (*m*/*z*): 385 $[M+H]^+$.

(*E*)-1-((2-(4-hydroxyphenyl)-1H-indol-3-yl)methylene)-4-p-tolylthiosemicarbazide (6i) Cream to yellow powder; Mp: 234–236 °C; Yield: 75%; ^{1}H NMR (500 MHz, DMSO-d_6, 25 °C, TMS) (δ, ppm): 2.32 (s, 3H; CH_3), 6.96 (d, $J=8.0$ Hz, 2H; $H_{3',5'}$), 7.13–7.21 (m, 4H; $H_{6,7,3'',5''}$), 7.40 (d, $J=7.7$ Hz, 1H; H_8), 7.47–7.52 (m, 4H; $H_{2',6',2'',6''}$), 8.29 (d, $J=7.7$ Hz, 1H; H_5), 8.54 (s, 1H; H–C=N), 9.44 (s, 1H; NH–Ph),

9.89 (s, 1H; OH), 11.48 (s, 1H; NH–C=S), 11.77 (s, 1H; NH-indole); ^{13}C NMR (DMSO-d_6, 25 °C, TMS) (δ, ppm): 20.7, 106.3, 111.3, 115.8, 121.0, 121.6, 122.3, 122.7, 125.0, 125.3, 128.7, 130.7, 134.1, 136.4, 136.7, 142.3, 143.5, 158.3, 174.2; IR (KBr, cm^{-1}): 3362 (N–H stretching), 3243 (OH), 3159 (Aromatic C–H), 1606 (C=N), 1553 (C=C), 1270 (C–N), 1206 (C=S), 1179 (C–O); Anal. Calcd. for $C_{23}H_{20}N_4OS$: C 68.98, H 5.03, N 13.99, Found: C 68.86, H 4.96, N 13.90; ESI–MS (*m*/*z*): 430 $[M+H]^+$.

(*E*)-1-((2-(4-methoxyphenyl)-1H-indol-3-yl)methylene)-4-p-tolylthiosemicarbazide (6j) Cream powder; Mp: 244–246 °C; Yield: 77%; ^{1}H NMR (500 MHz, DMSO-d_6, 25 °C, TMS) (δ, ppm): 2.31 (s, 3H; CH_3), 3.85 (s, 3H; OCH_3), 7.14-7.23 (m, 6H; $H_{3',5',3'',5'',6,7}$), 7.43 (d, J = 7.7 Hz, 1H; H_8), 7.52 (d, J = 7.5 Hz, 2H; $H_{2'',6''}$), 7.60 (d, J = 8.0 Hz, 2H; $H_{2',6'}$), 8.31 (d, J = 7.7 Hz, 1H; H_5), 8.55 (s, 1H; H–C=N), 9.45 (s, 1H; NH–Ph), 11.50 (s, 1H; NH–C=S), 11.84 (s, 1H; NH-indole). ^{13}C NMR (DMSO-d_6, 25 °C, TMS) (δ, ppm): 20.3, 55.3, 106.7, 111.3, 111.4, 114.3, 114.4, 123.2, 124.7, 124.8, 125.2, 128.5, 128.6, 130.6, 134.0, 136.7, 142.0, 142.8, 159.8, 174.3; IR (KBr, cm^{-1}): 3360, 3307 (N–H stretching), 3186 (Aromatic C–H), 1607 (C=N), 1544 (C=C), 1273 (C–N), 1202 (C=S), 1182 (C–O); Anal. Calcd. for $C_{24}H_{22}N_4OS$: C 69.54, H 5.35, N 13.52, Found: C 69.39, H 5.28, N 13.47; ESI–MS (*m*/*z*): 444 $[M+H]^+$.

(*E*)-1-((2-(4-chlorophenyl)-1H-indol-3-yl)methylene)-4-p-tolylthiosemicarbazide (6k) Yellow to light green powder; Mp: 239–242 °C; Yield: 82%; ^{1}H NMR (500 MHz, DMSO-d_6, 25 °C, TMS) (δ, ppm): 2.31 (s, 3H; CH_3), 7.17–7.18 (m, 3H; $H_{3'',5'',6}$), 7.25 (t, J = 7.8, 1H; H_7), 7.45 (d, J = 7.8 Hz, 1H; H_8), 7.49 (d, J = 8.0 Hz, 2H; $H_{3',5'}$), 7.65–7.69 (m, 4H; $H_{2',6',2'',6''}$), 8.36 (d, J = 7.8 Hz, 1H; H_5), 8.54 (s, 1H; H–C=N), 9.49 (s, 1H; NH–Ph), 11.51 (s, 1H; NH–C=S), 12.03 (s, 1H; NH-indole); ^{13}C NMR (DMSO-d_6, 25 °C, TMS) (δ, ppm): 21.6, 106.9, 111.3, 116.8, 123.4, 124.5, 126.1, 128, 129.6, 130.4, 132.7, 133.5, 135.4, 135.7, 137.6, 138.0, 138.1, 140.8, 175.3; IR (KBr, cm^{-1}): 3346, 3315 (N–H stretching), 3142 (Aromatic C–H), 1607 (C=N), 1544 (C=C), 1272 (C–N), 1203 (C=S); Anal. Calcd. for $C_{23}H_{19}ClN_4S$: C 65.94, H 4.57, N 13.37, Found: C 65.91, H 4.61, N 13.35; ESI–MS (*m*/*z*): 448 $[M+H]^+$.

(*E*)-1-((2-(4-bromophenyl)-1H-indol-3-yl)methylene)-4-p-tolylthiosemicarbazide (6l) Yellow to light green powder; Mp > 250 °C; Yield: 80%; ^{1}H NMR (500 MHz, DMSO-d_6, 25 °C, TMS) (δ, ppm): 2.31 (s, 3H; CH_3), 7.17–7.18 (m, 3H; $H_{3'',5'',6}$), 7.25 (t, J = 7.8 Hz, 1H; H_7), 7.45 (d, J = 7.8 Hz, 1H; H_8), 7.49 (d, J = 8.1 Hz, 2H; $H_{3',5'}$), 7.61 (d, J = 8.2 Hz, 2H; $H_{2'',6''}$), 7.79 (d, J = 8.1 Hz, 2H; $H_{2',6'}$), 8.36 (d, J = 7.8 Hz, 1H; H_5), 8.54 (s, 1H; H–C=N), 9.48 (s, 1H; NH–Ph), 11.50 (s, 1H; NH–C=S), 12.02 (s, 1H; NH-indole); ^{13}C NMR (DMSO-d_6, 25 °C, TMS) (δ, ppm): 20.9, 107.8, 111.6, 121.2, 122.4, 122.7, 123.4, 125.1, 125.2, 128.7, 130.1, 131.3, 131.9, 134.2, 136.6, 136.7, 141.2, 141.5, 174.50; IR (KBr, cm^{-1}): 3431, 3342 (N–H stretching), 3141 (Aromatic C–H), 1593 (C=N), 1542 (C=C), 1273 (C–N), 1202

(C=S); Anal. Calcd. for $C_{23}H_{19}BrN_4S$: C 59.61, H 4.13, N 12.09, Found: C 59.72, H 4.21, N 12.18; ESI–MS (*m*/*z*): 494 $[M+H]^+$.

(*E*)-1-((2-(4-hydroxyphenyl)-1H-indol-3-yl)methylene)-4-methylthiosemicarbazide (6m) Cream powder; Mp > 250 °C; Yield: 83%; ^{1}H NMR (500 MHz, DMSO-d_6, 25 °C, TMS) (δ, ppm): 3.09 (d, $J=4$ Hz, 3H; CH_3), 6.94 (d, $J=8.3$ Hz, 2H; $H_{3',5'}$), 7.14 (t, $J=7.6$ Hz, 1H; H_6), 7.20 (t, $J=7.6$ Hz, 1H; H_7), 7.38 (d, $J=7.6$ Hz, 1H; H_8), 7.44 (d, $J=8.3$ Hz, 2H; $H_{2',6'}$), 7.80–7.86 (m, 1H; $NHCH_3$), 8.33 (d, $J=7.6$ Hz, 1H; H_5), 8.44 (s, 1H; H–C=N), 9.86 (s, 1H; OH), 11.11 (s, 1H; NH–C=S), 11.68 (s, 1H; NH-indole); ^{13}C NMR (DMSO-d_6, 25 °C, TMS) (δ, ppm): 31.2, 106.5, 111.2, 115.7, 120.8, 121.7, 122.6, 122.7, 125.3, 130.7, 136.2, 141.5, 142.9, 158.2, 176.6; IR (KBr, cm^{-1}): 3359 (N–H stretching), 3243 (OH), 3141 (Aromatic C–H), 1605 (C=N), 1553 (C=C), 1271 (C–N), 1234 (C=S), 1180 (C–O); Anal. Calcd. for $C_{17}H_{16}N_4OS$: C 62.94, H 4.97, N 17.27, Found: C 62.83, H 5.05, N 17.19; ESI–MS (*m*/*z*): 325 $[M+H]^+$.

(*E*)-1-((2-(4-methoxyphenyl)-1H-indol-3-yl)methylene)-4-methylthiosemicarbazide (6n) Dark cream; Mp: 229–230 °C; Yield: 79%; ^{1}H NMR (500 MHz, DMSO-d_6, 25 °C, TMS) (δ, ppm): 3.08 (d, $J=4.4$ Hz, 3H; CH_3), 3.85 (s, 3H; OCH_3), 7.12–7.17 (m, 3H; $H_{3',5',6}$), 7.21 (t, $J=7.7$ Hz, 1H; H_7), 7.40 (d, $J=7.7$ Hz, 1H; H_8), 7.56 (d, $J=8.5$ Hz, 2H; $H_{2',6'}$), 7.83–7.87 (m, 1H; $NHCH_3$), 8.35 (d, $J=7.7$ Hz, 1H; H_5), 8.45 (s, 1H; H–C=N), 11.13 (s, 1H; NH–C=S), 11.76 (s, 1H; NH-indole); ^{13}C NMR (DMSO-d_6, 25 °C, TMS) (δ, ppm): 31.3, 55.6, 106.9, 111.5, 114.4, 121.0, 122.9, 123.3, 125.1, 127.8, 130.6, 136.3, 141.5, 142.4, 159.7, 176.5; IR (KBr, cm^{-1}): 3345, 3201 (N–H stretching), 3159 (Aromatic C–H), 1609 (C=N), 1544 (C=C), 1275 (C–N), 1242 (C=S), 1176 (C–O); Anal. Calcd. for $C_{18}H_{18}N_4OS$: C 63.88, H 5.36, N 16.56, Found: C 63.97, H 5.41, N 16.61; ESI–MS (*m*/*z*): 339 $[M+H]^+$.

(*E*)-1-((2-(4-chlorophenyl)-1H-indol-3-yl)methylene)-4-methylthiosemicarbazide (6o) Yellow powder; Mp: 235–237 °C; Yield: 84%; ^{1}H NMR (500 MHz, DMSO-d_6, 25 °C, TMS) (δ, ppm): 3.08 (d, $J=4.3$ Hz, 3H; CH_3), 7.18 (t, $J=7.7$ Hz, 1H; H_6), 7.25 (t, $J=7.7$ Hz, 1H; H_7), 7.43 (d, $J=7.7$ Hz, 1H; H_8), 7.60–7.67 (m, 4H; $H_{3',5',2',6'}$), 7.85–7.93 (m, 1H; $NHCH_3$), 8.39 (d, $J=7.7$ Hz, 1H; H_5), 8.45 (s, 1H; H–C=N), 11.14 (s, 1H; NH–C=S), 11.94 (s, 1H; NH-indole); ^{13}C NMR (DMSO-d_6, 25 °C, TMS) (δ, ppm): 31.2, 107.9, 111.5, 121.1, 123.0, 123.3, 125.0, 128.9, 129.8, 130.9, 133.5, 136.5, 140.6, 140.9, 176.9; IR (KBr, cm^{-1}): 3383, 3305 (N–H stretching), 3161 (Aromatic C–H), 1597 (C=N), 1546 (C=C), 1269 (C–N), 1238 (C=S); Anal. Calcd. for $C_{17}H_{15}ClN_4S$: C 59.56, H 4.41, N 16.34, Found: C 59.47, H 4.36, N, 16.28; ESI–MS (*m*/*z*): 343 $[M+H]^+$.

(E)-1-((2-(4-bromophenyl)-1H-indol-3-yl)methylene)-4-methylthiosemicarbazide (6p) Dark yellow powder; Mp: 242–244 °C; Yield: 83%; ^{1}H NMR (500 MHz, DMSO-d_6, 25 °C, TMS) (δ, ppm): 3.08 (d, $J=4.4$ Hz, 3H; CH_3), 7.18 (t, $J=7.8$ Hz, 1H; H_6), 7.25 (t, $J=7.8$ Hz, 1H; H_7), 7.43 (d, $J=7.8$ Hz, 1H; H_8), 7.57 (d, $J=8.3$ Hz, 2H; $H_{3',5'}$), 7.77 (d, $J=8.3$ Hz, 2H; $H_{2',6'}$), 7.86–7.91 (m, 1H; $NHCH_3$),

8.39 (d, $J = 7.8$ Hz, 1H; H_5), 8.45 (s, 1H; H–C=N), 11.13 (s, 1H; NH–C=S), 11.93 (s, 1H; NH-indole); ^{13}C (DMSO-d_6, 25 °C, TMS) (δ, ppm): 31.1, 108.0, 111.5, 121.1, 122.2, 122.9, 123.0, 123.3, 125.0, 130.1, 131.2, 131.8, 136.5, 140.7, 176.7; IR (KBr, cm^{-1}): 3387, 3303 (N–H stretching), 3161 (Aromatic C–H), 1597 (C=N), 1552 (C=C), 1272 (C–N), 1237 (C=S); Anal. Calcd. for $C_{17}H_{15}BrN_4S$: C 52.72, H 3.90, N 14.47, Found C 52.65, H 3.86, N 14.41; ESI–MS (*m*/*z*): 389 $[M+H]^+$.

Biology

Anti-proliferative assay

The cytotoxic activity of synthesized compounds **6a–p** was assessed against three different cancer cell lines [38]. Tumor cell lines including lung cancer cell line (*A-549*), liver cancer cell line (*Hep-G2*), and breast cancer cell line (*MCF-7*) were obtained from the National Cell Bank of Iran and grown in RPMI-1640 medium (Gibco, UK). Exponentially growing cells (1×10^4 cells/well) were seeded in 96-well plates in RPMI1640 medium at 37 °C under 5% CO_2 supplemented with 10% FBS, 1% L-glutamine, and penicillin-streptomycin and incubated overnight. The cells were treated by different concentrations of test compounds and allowed to incubate for 48 h in a humidified atmosphere. All compounds were initially dissolved in DMSO, and the final concentration of DMSO was less than 1% in all concentration of the applied compounds. Etoposide and colchicine were used as the positive control in this experiment. After 48 h further incubation, the medium was replaced with MTT (1 mg/mL) and followed by 4-h incubation. After formation of blue formazan crystals, the culture medium was replaced with 100 µL of DMSO and absorbance values were measured using a multi-well plate reader (Gen5, Epoch, BioTek, America) at 492 nm wavelengths. The IC_{50} values were compared with the control and expressed in mean ± SD from the dose–response logarithmic curves of at least three independent experiments.

Acridine orange/ethidium bromide double staining

Apoptosis in treated cancer cells was determined morphologically after staining with acridine orange/ethidium bromide (AO/EB) using fluorescence microscopy [37]. *A-549* cell grown in 12 well plates (5×10^5 cells/well) were treated with and without IC_{50} concentrations of compound **6n** for 24 h. Then the cells were washed for three times with PBS. Finally, ethidium bromide/acridin orange (1:1, 100 mg/mL) solution was added to the cell suspension, and the nuclear morphology was evaluated by fluorescence microscopy (Zeiss, Germany). All experiments were repeated three times.

Flow cytometry analysis of the apoptotic cells with Annexin V-FITC/PI staining

Flow cytometry analyses for **6n** were performed to confirm apoptosis induced in comparison with standard drug etoposide. In brief, 5×10^5 cells/well of *A-549* cells was treated with IC_{50} dose of most potent compound **6n**. After 24 h, the cells were washed twice with cold PBS, collected by centrifugation and resuspended in

1 × annexin V binding buffer (0.1 M Hepes/NaOH (pH 7.4), 1.4 M NaCl, 25 mM $CaCl_2$). Then, the cells were double stained with Annexin V-FITC and 5 µL of PI, and the cells were gently vortex and incubated at room temperature for 15 min in the dark before flow cytometry. Finally, 400 µL of 1x annexin binding buffer was added into the suspension, and the cells were analyzed using a flow cytometer within 1 h.

Antioxidant activity

The DPPH antioxidant activities of **6a–p** were evaluated according to the literature [39, 40]. The DPPH solution (6.25×10^{-5} M) was prepared in methanol. Then different sample solutions of compounds **6a–p** (2000, 1000, 500, 250, and 125 µg mL^{-1}) were obtained in methanol. Subsequently, 0.1 mL of each compound solution was added to 3.9 mL of DPPH solution and was shaken vigorously. The mixture was allowed to stand at room temperature in dark for 30 min, and their absorbance was measured at 517 nm. Ascorbic acid was used as the reference standard. The control sample contained all the reagents except the test compound, and methanol was used as the blank. The percentage of radical scavenging activity was calculated as follows:

Radical scavenging activity $(\%) = [(A_{\text{control}} - A_{\text{sample}})/A_{\text{control}}] \times 100$, where A_{control} is the absorbance of the control reaction, and A_{sample} is the absorbance in the presence of the compounds or standard absorbance of the test compounds. The IC_{50} values for the sample compounds were determined by plotting the radical scavenging activity percentage versus the concentration of the sample compound.

Molecular docking

A docking study by using the Discovery Studio 4.1 (DS4.1) were performed to understand the binding modes of the compounds with tubulin and ATPase domain of topoisomerase IIα crystal structure.

For ligand preparation, all the molecular structures were sketched in the ChemDraw ultra 8.0 program, and were shifted into the Discovery Studio 4.1 (DS4.1) for minimization. The compounds were then typed with a CHARMm force field, the partial charges were computed by the Momany–Rone option [41]. A minimizer algorithm was used to minimize the resulting structures, that carried out 1000 steps of the steepest descent with a RMS gradient tolerance of three followed by a conjugate gradient minimization. The intended crystal protein structures were extracted from the protein data bank (www.rcsb.org) (PDB ID: 1S0 [21] and 1ZXM [30] for tubulin and topoisomerase II, respectively). All protein preparations and minimizations were done using the protocols in DS4.1. The region of interest used for GOLD docking was defined as when all the protein residues were within the 8.96 Å and 10 Å of the reference ligands of tubulin and topoisomerase IIα, respectively. The C and D chains were eliminated from the structure of tubulin and chain A was selected for the docking study In the structure of topoisomerase IIα. All bound water molecules and ligands were removed from the proteins, non-polar hydrogen atoms were merged and the polar hydrogen atoms were added. At the beginning of the docking, it is essential to validate the docking reliability. The ligands colchicine and

ANP were re-docked to the bonding site of tubulin and topoisomerase, respectively. The docked conformation of colchicine and ANP using Gold showed similar binding poses with the original X-ray structure with the root mean of square deviation (rmsd) of 0.51 and 0.89 for colchicine and ANP, respectively. Therefore, the docking protocol could be extended to inspect the binding modes of the corresponding compound into the tubulin and ATPase domain of topoisomerase II using GOLD 5.3.0. The annealing parameters of the Van der Waals and hydrogen bonding interactions were 6.0 and 3.0 Å, respectively. All the other parameters were saved at their default values for the docking study. Gold flexible ligand docking generated 10 positions of each ligand, which were ranked using the Goldscore function. The top ranked pose with highest Goldscore fitness was analyzed using Accelrys Discovery studio to reveal the hydrogen bond interaction and binding mode within the binding domain.

Calculation of logP

The cLogP values for the synthesized series six compounds as well as etoposide and colchicine were calculated using Molinspiration webME Editor 1.16 [42] in order to measure their lipophilicity (Table 1).

Acknowledgements This work was supported by Grants from Isfahan university of Medical Sciences and Tehran University of Medical Sciences.

Compliance with ethical standards

Conflict of interest The authors declare that they have no conflict of interests.

References

1. X. Zhang, K.P. Rakesh, C.S. Shantharam, H.M. Manukumar, A.M. Asiri, H.M. Marwani, H.L. Qin, Bioorg. Med. Chem. **26**, 340 (2017)
2. G.F. Zha, H.L. Qin, B.G.M. Youssif, M.W. Amjad, M.A.G. Raja, A.H. Abdelazeem, S.N.A. Bukhari, Eur. J. Med. Chem. **135**, 34 (2017)
3. H.L. Qin, M.A. Ghafoor Raja, L. Jing, B.G.M. Youssif, M.W. Amjad, S.N.A. Bukhari, M.A. Hussain, Z. Hussain, S.N. Kazmi, Chem. Biol. Drug Des. **90**(3), 443 (2017)
4. J.F. de Oliveira, T.S. Lima, D.B. Vendramini-Costa, S.C.B. de Lacerda Pedrosa, E.A. Lafayette, R.M.F. da Silva, S.M.V. de Almeida, R.O. de Moura, A.L.T.G. Ruiz, J. Ernesto de Carvalho, M.C. Alves de Lima, Eur. J. Med. Chem. **136**, 305 (2017)
5. J.F. de Oliveira, A.L. da Silva, D.B. Vendramini-Costa, C.A. da Cruz Amorim, J.F. Campos, A.G. Ribeiro, R.O. de Moura, J.L. Neves, A.L.T.G. Ruiz, J.E. de Carvalho, M.D.C.A. de Lima, Eur. J. Med. Chem. **104**, 148 (2015)
6. P.R. Kamath, D. Sunil, A.A. Ajees, K.S.R.S. Pai, Bioorg. Chem. **63**, 101 (2015)
7. A. Negi, J.M. Alex, S.M. Amrutkar, A.T. Baviskar, G. Joshi, S. Singh, U.C. Banerjee, R. Kumar, Bioorg. Med. Chem. **23**, 5654 (2015)
8. C. Zhao, K.P. Rakesh, S. Mumtaz, B. Moku, A.M. Asiri, H.M. Marwani, H.M. Manukumar, H.L. Qin, RSC Adv. **8**, 9487 (2018)
9. K.P. Rakesh, C.S. Shantharam, M.B. Sridhara, H.M. Manukumar, H.L. Qin, Med. Chem. Commun. **8**, 2023 (2017)
10. H.L. Qin, Z.P. Shang, I. Jantan, O.U. Tan, M.A. Hussain, M. Sher, S.N.A.Bukhari, RSC Adv. **5**, 46330 (2015)
11. C. Zhao, K. Rakesh, L. Ravidar, W.Y. Fang, Eur. J. Med. Chem. **162**, 679 (2019)

12. K.P. Rakesh, S.M. Wang, J. Leng, L. Ravindar, A.M. Asiri, H.M. Marwani, H.L. Qin, Anticancer Agents Med. Chem. **18**(4), 488 (2018)
13. S.M. Wang, G.F. Zha, K.P. Rakesh, N. Darshini, T. Shubhavathi, H.K. Vivek, N. Mallesha, H.L. Qin, Med. Chem. Commun. **8**, 1173 (2017)
14. H.L. Qin, J. Leng, C.P. Zhang, I. Jantan, M.W. Amjad, M. Sher, M. Naeem-ul-Hassan, M.A. Hussain, S.N.A. Bukhari, J. Med. Chem. **59**(7), 3549 (2016)
15. A. Ozdemir, M.D. Altıntop, G. Turan-Zitouni, G.A. Çiftçi, I. Ertorun, O. Alatas, Z.A. Kaplancıklı, Eur. J. Med. Chem. **89**, 304 (2015)
16. M. Zhang, Q. Chen, G. Yang, Eur. J. Med. Chem. **89**, 421 (2015)
17. N.T. Tzvetkov, S. Hinz, P. Küppers, M. Gastreich, C.E. Müller, J. Med. Chem. **57**(15), 6679 (2014)
18. S. Kumar, S. Mehndiratta, K. Nepali, M.K. Gupta, S. Koul, P.R. Sharma, A.K. Saxena, K.L. Dhar, Org. Med. Chem. Lett. **3**(1), 3 (2017)
19. Z. Datong, X. Rongrong, G. Shoudong, Z. Yaling, Res. Chem. Intermed. **41**(9), 6575 (2015)
20. G. De Martino, M.C. Edler, G. La Regina, A. Coluccia, M.C. Barbera, D. Barrow, R.I. Nicholson, G. Chiosis, G. La Regina, A. Brancale, A. Coluccia, E. Hamel, M. Artico, R. Silvestri, J. Med. Chem. **49**, 947 (2006)
21. S.N. Baytas, N. Inceler, A. Yılmaz, A. Olgac, E. Banoglu, E. Hamel, R. Bortolozzi, G. Viola, S. Menevse, Bioorg. Med. Chem. **22**, 3096 (2014)
22. R.S. Patil, A. Patil, K.D. Beaman, S.A. Patil, Future Med. Chem. **8**(11), 1291 (2016)
23. R. Gastpar, M. Goldbrunner, D. Marko, E. Angerer, J. Med. Chem. **41**, 4965 (1998)
24. D. Kaufmann, M. Pojarova, S. Vogel, R. Liebl, R. Gastpar, D. Gross, T. Nishino, T. Pfaller, E. Angerer, Bioorg. Med. Chem. **15**, 5122 (2007)
25. E.A. Britta, D.B. Scariot, H. Falzirolli, T. Ueda-Nakamura, C.C. Silva, B.P. Dias Filho, R. Borsali, C.V. Nakamura, BMC Microbiol. **14**, 236 (2014)
26. M.A. Souza, S. Juhann, L.A.R.D.S. Lima, F.F. Campos, I.C. Mendes, H. Beraldo, E.M.D. Souza-Fagundes, P.S. Cisalpino, C.A. Rosa, T.M.D.A. Alves, N.P.D. Sa, C.L. Zani, Mem. Inst. Oswaldo Cruz **108**(3), 342 (2013)
27. A.S. Salman, N.A. Mahmoud, M.A. Mohamed, A. Abdel-Aziem, D.M. Elsisi, Am. J. Org. Chem. **6**(2), 39 (2016)
28. S.M.V. de Almeida, E.A. Lafayette, L.P.B.G. da Silva, C.A.D.C. Amorim, T.B. de Oliveira, A.L.T.G. Ruiz, J.E. de Carvalho, R.O. de Moura, E.I.C. Beltrão, M.D.C.A. de Lima, L.B.D.C. Júnior, Int. J. Mol. Sci. **16**, 13023 (2015)
29. B. Xu, Y. Yu, P. Wan, Res. Chem. Intermed. **40**, 3095 (2014)
30. H. Huang, Q. Chen, X. Ku, L. Meng, L. Lin, X. Wang, C. Zhu, Y. Wang, Z. Chen, M. Li, H. Jiang, K. Chen, J. Ding, H. Liu, J. Med. Chem. **53**, 3048 (2010)
31. C. Karaaslan, H. Kadri, T. Coban, S. Suzen, Bioorg. Med. Chem. Lett. **23**, 2671 (2013)
32. V. Mashayekhi, K. Haj Mohammad Ebrahim Tehrani, P. Azerang, S. Sardari, F. Kobarfard, Arch. Pharmacal. Res. 1 (2013)
33. Z. Liu, S. Wu, Y. Wang, R. Li, J. Wang, L. Wang, Y. Zhao, P. Gong, Eur. J. Med. Chem. **87**, 782 (2014)
34. M. Safavi, N. Esmati, S.K. Ardestani, S. Emami, S. Ajdari, J. Davoodi, A. Shafiee, A. Foroumadi, Eur. J. Med. Chem. **58**, 573 (2012)
35. A.H. Halawa, A.A.E.H. Hassan, M.A. El-Nassag, M.M.A. El-All, G.E.R.A. El-Jaleel, E.M. Eliwa, A.H. Bedair, Eur. J. Chem. **5**(1), 111 (2014)
36. N. Liang, D.D. Kitts, Molecules **19**, 19180 (2014)
37. S. Sepehri, S. Soleymani, R. Zabihollahi, M.R. Aghasadeghi, M. Sadat, L. Saghaie, A. Fassihi, Chem. Biodivers. **14**, e1700295 (2017)
38. M. Safavi, A. Ashtari, F. Khalili, S.S. Mirfazli, M. Saeedi, S. Ardestani, K.P. Ranjbar, R.M.B. Tehrani, B. Larijani, M. Mahdavi, Chem. Biol. Drug Des. **92**, 1373 (2018)
39. M. Volovenko, E.V. Resnyanska, Mendel Commun. **12**, 119 (2002)
40. N. Mahmoodi, S. Ghodsi, Res. Chem. Intermed. **43**(2), 661 (2017)
41. F.A. Momany, R. Rone, J. Comput. Chem. **13**, 888 (1992)
42. http://www.molinspiration.com/cgi-bin/properties

Affiliations

Zohreh Bakherad[1] · Maliheh Safavi[2] · Afshin Fassihi[1] · Hojjat Sadeghi-Aliabadi[1] · Mohammad Bakherad[3] · Hossein Rastegar[4] · Jahan B. Ghasemi[5] · Saghi Sepehri[6] · Lotfollah Saghaie[1] · Mohammad Mahdavi[7]

1 Department of Medicinal Chemistry, School of Pharmacy and Pharmaceutical Sciences, Isfahan University of Medical Sciences, Isfahan 81746-73461, Iran

2 Department of Biotechnology, Iranian Research Organization for Science and Technology, Tehran 33535-111, Iran

3 School of Chemistry, Shahrood University of Technology, Shahrood, Iran

4 Food and Drug Control Laboratories, Food and Drug Laboratory Research Center, MOE and ME, Tehran, Iran

5 Drug Design in Silico Lab, Chemistry Faculty, School of Sciences, University of Tehran, Teheran, Iran

6 Department of Medicinal Chemistry, School of Pharmacy, Ardabil University of Medical Sciences, Ardabil 5618953141, Iran

7 Endocrinology and Metabolism Research Center, Endocrinology and Metabolism Research Institute, Tehran University of Medical Sciences, Tehran, Iran